Thermodynamic and Kinetic Stability of Coherent Germanium Nanocrystallites in a Silicon Host

by

Shuba Balasubramanian

Submitted to the Department of Materials Science and Engineering
in partial fulfillment of the requirements for the degree of

Master of Science in Materials Science and Engineering

at the

MASSACHUSETTS INSTITUTE OF TECHNOLOGY

June 1996

Author .....
Department of Materials Science and Engineering
May 7, 1996

Certified by .....
Kirk D. Kolenbrander
Associate Professor of Electronic Materials
Thesis Supervisor

Certified by .....
Gerbrand Ceder
Associate Professor of Materials Science and Engineering
Thesis Supervisor

Accepted by .....
Michael F. Rubner
Chair, Departmental Committee on Graduate Students

To My Mother

Thermodynamic and Kinetic Stability of Coherent Germanium Nanocrystallites in a Silicon Host

by

Shuba Balasubramanian

Submitted to the Department of Materials Science and Engineering
on May 7, 1996, in partial fulfillment of the
requirements for the degree of
Master of Science in Materials Science and Engineering

Abstract

The thermodynamic stability range of coherent Ge quantum dots capped with an epitaxial Si shell is studied. The critical radius is evaluated as a function of Si shell thickness and ge nanocrystallite radius by comparing the energy of the system in the coherent and incoherent state. The system is found to remain coherent up to a Ge nanocrystallite radius of about 100 Å, irrespective of the Si shell thickness. Nanocrystallites of radii larger than 270 Å lose coherency by the generation of perfect dislocation loops. In nanocrystallites of intermediate radii (between 100 Å and 270 Å), the coherency is lost by the introduction of partial dislocation loops enclosing a stacking fault. As the shell thickness decreases, the critical radius increases.

Further, the kinetics of inter-diffusion of the Ge nanocrystallite with the Si host is studied. A multi-body empirical potential model, derived from ab-initio pseudo-potential calculations, is used to calculate the activation energy for interdiffusion by the concerted exchange mechanism. The activation energy is found to be dependent on the atomic environment and the strain due to the nanocrystallite.

Using this model, we find that the activation energy can be calculated accurately (to within 0.01 eV) by considering only the chemical identity and arrangement of the atoms in the first and second neighbor shells. Depending on the first neighbor atomic environment the activation energies could differ by 0.2 to 0.4 eV. The effect of second neighbor environment on activation energy follows the same trend as the effect of first neighbors, but is of a smaller magnitude (0.07 eV). The activation energy is also dependent on the long range chemical identity of the diffusing medium. The relative effect of these parameters on activation energy has been clearly established. These effects of atomic environment on activation energy are applicable to any Si-Ge diffusion by the concerted exchange mechanism.

In the coherent nanocrystallite/host system, in addition to these effects, strain is found to play an important role. Even for systems with the same atomic environment, the activation energy is anisotropic with respect to the direction in which the atoms exchange relative to the radial direction from the center of the nanocrystallite. The activation energy for a radial exchange is lower than that for a tangential exchange

by 0.4 eV. This strain induced anisotropy in activation energy decreases to 0.05 eV as the distance from the interface increases.

Thesis Supervisor: Kirk D. Kolenbrander
Title: Associate Professor of Electronic Materials

Thesis Supervisor: Gerbrand Ceder
Title: Associate Professor of Materials Science and Engineering

Acknowledgments

I am grateful to my advisors Prof. Kirk D. Kolenbrander and Prof. Gerbrand Ceder who have shown a lot of trust in me and have been a constant source of inspiration. I thank Prof. Robert W. Balluffi for useful discussions on dislocation theory.

I am indebted to my good friends Patrick (Pumpkin) Tepesch, Gerardo (Jerry) Garbulsky, Adrian (Adro) Kohan, Kadri Aydinol, Anton Van Der Ven and Axel Vandewalle on whom I could always rely on. I consider myself extremely lucky to have had the opportunity to work with them. I thank Arun Seraphin, Eric Werwa, Tracey Burr and Shih-Tung Ngiam for providing moral support at times when I needed it most. My sister, Uma Subramaniam and my good friend, Ram Ratnagiri have always been there for me. Each and everyone of the above people, individually and collectively, have contributed to making my stay here at MIT, the best two years of my life.

To my guru and parents, I owe everything I am today. Without their caring support and encouragement I would not have attempted to embark on such an ambitious project.

Shuba Balasubramanian

Contents

List of Figures

List of Tables

Chapter 1

Introduction

One-dimensionally quantum confined semiconductor thin film ("quantum well") structures have emerged as important materials systems in today's microelectronic and optoelectronic technologies. These lattice mismatched thin film heterostructures rely on the difference in bandgap of the semiconductors to attain quantum confinement. A critical factor in the technological success of these strained layer epitaxial systems lies in the ability to grow coherent interfaces without defects, as these defects are generally detrimental to electrical and optical properties.

Recently, experimental advances in materials processing have permitted the fabrication of three-dimensionally quantum confined semiconductor nanocrystallite ("quantum dot") systems positioned within semiconductor host materials [10, 11, 12]. Nanocrystallites ("quantum dots") are semiconductor crystallites in the 1-10 nm diameter range consisting of hundreds to thousands of atoms with bulk bonding geometry. These materials represent the three-dimensionally confined analogs to quantum well heterostructures. As with quantum wells, lattice coherency at the dot/host interface holds a key in defining the electronic, optoelectronic, and photonic characteristics of these heterostructures. Imperfections around the interface can arise from lattice imperfections (misfit dislocations) or from interdiffusion of atoms between the nanocrystallite and the host.

It is very difficult to experimentally study the nature of the interface. Now, with the availability of faster computers, it is possible to gain an understanding into the

stability of the interface between the nanocrystallite and the host. In this thesis, we study the interface between a Ge nanocrystallite and a Si host.

In Chapter 2, we calculate a lower bound for the critical radius of the Ge nanocrystallite in a Si host. The energy of the system in the coherent state and the incoherent state is calculated from elasticity theory. The critical radius is calculated by setting the two energies to be equal. We find that very large nanocrystallites can be grown coherently without the generation of dislocations.

In Chapter 3, we study the interdiffusion of Ge and Si on the atomic scale by the concerted exchange mechanism. We develop a multi-body empirical potential model to calculate the activation energy for interdiffusion. Using this model, we show the dependence of activation energy on various parameters such as atomic environment and strain. With this knowledge, it would be possible to simulate the diffusion of the interface.

Chapter 2

Three-Dimensional Epitaxy : Thermodynamic Stability Range of Coherent Germanium Nanocrystallites in Silicon

2.1 Introduction

Theoretical treatments to describe the epitaxial relationships observed on mismatched thin film systems ("quantum wells") are well developed. This extensive literature builds on the pioneering efforts of Frank and van der Merwe [1, 2, 3, 4, 5, 6],and Jesser and Matthews [7, 8, 9] who predicted that a coherent epilayer of a crystal can be grown on a substrate of different lattice parameter. A direct result of these efforts is the community's present understanding of the concept of a "critical thickness" that defines the maximum size at which the misfitting layer remains coherent with the host matrix.

As with quantum wells, in quantum dots the lattice coherency at the dot/host interface holds a key in defining the electronic, optoelectronic, and photonic characteristics of these heterostructures. A theoretical understanding of the morphological

limits of three-dimensional epitaxy in these systems is needed to accompany the experimental efforts as the promise of quantum dot materials is further explored. An appropriate first step is the determination of a "critical radius" that describes the largest sphere that can be coherently supported in a mismatched system of nanocrystallite and host.

Although nanocrystallite structures have to date not been studied from a point of view of coherency, the conditions under which a precipitate is coherent with its matrix has been known by the metallurgical community for many decades. In 1940, Nabarro [14, 15] determined the elastic strains developed when a precipitate is formed in an alloy. Nabarro [15], Jesser [16], Brown [17, 18] and others calculated the critical size of precipitates. Brown [17] considered the interaction of one dislocation with coherent spherical precipitates and evaluated the critical size from a thermodynamic point of view.

We present here the first effort to describe the critical limits of epitaxy for three dimensionally confined nanocrystallites in a crystalline host. Building simultaneously on the principles of the quantum well strained layer epitaxy and on the understanding of coherent precipitates in alloys, we have calculated the critical radius of a semiconductor of different lattice parameter. We choose as our representative system the epitaxial positioning of Ge nanocrystallites in a crystalline Si host.

2.2 Thermodynamic Considerations

The lattice parameter of bulk Ge is approximately 4% larger than that of Si. When a thick Si shell is grown epitaxially on a Ge nanocrystallite of bulk lattice parameter, the lattice misfit causes coherency strains to develop in the system. As the radius of the nanocrystallite increases, the stress increases and reaches a stage where the misfit strain can no longer be accommodated coherently. At this point coherency is lost by the formation of defects (i.e., dislocations) and the system transforms to an incoherent state.

The coherent-to-incoherent transformation becomes thermodynamically favorable

if the total energy of the system after transformation is less than the total energy before transformation, i.e., $E_{Incoherent} \leq E_{Coherent}$. However, this is not the only requirement for this transformation to take place as the nucleation kinetics of the defect may play an important role. In planar epitaxy it is found that dislocation-free interfaces can be grown upto a film thicknesses 5 to 10 times larger than the critical thickness predicted by Matthews [19, 20] and Van der Merwe [1, 6]. This metastability in the system has been explained by the slow kinetics of the system and or the insensitivity of the experimental techniques used [21]. The thermodynamic critical radius which is determined in this thesis, can therefore be seen as the minimal radius at which Si capped Ge particles can be kept coherent.

At the critical radius, the energy of the system in the coherent state and incoherent state are equal. In the coherent state, the energy of the system is the elastic strain energy caused by the misfit,

$$E_{Coherent} = E_{Elastic} \tag{2.1}$$

In the incoherent state the stress field of the defect interacts with the stress field of the misfitting nanocrystallite and relieves part of the misfit strain, thereby releasing a part of the elastic strain energy, leaving a residual elastic energy. In addition, energy is required to create the defect. Therefore, the energy of the system in the incoherent state is,

$$E_{Incoherent} = E_{Residual\ Elastic} + E_{Defect} \tag{2.2}$$

In calculating these energy contributions, we assume that both nanocrystallite and shell materials are elastically isotropic and that the laws of continuum mechanics are applicable to the nanocrystallite/shell systems.

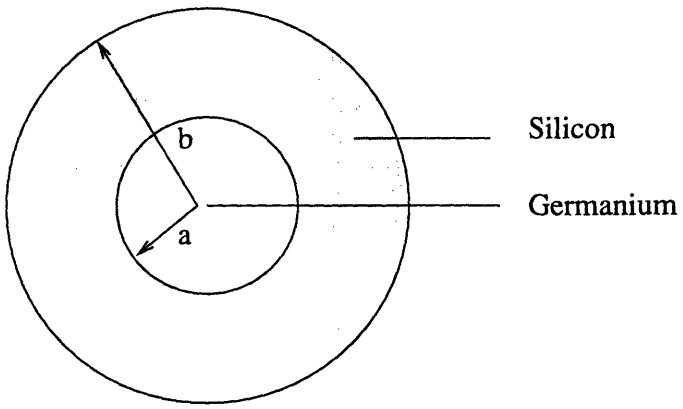

Figure 2-1: Schematic diagram: Ge nanocrystallite capped with Si shell

2.2.1 Coherent State

Elastic Strain Energy

We assume that the spherical Ge nanocrystallite is epitaxially capped with a concentric Si shell having the same orientation as the nanocrystallite. A schematic diagram of the system is shown in Fig. 2-1. The inner region, $0 < r < a$, is the Ge nanocrystallite and the outer region $a < r < b$ is the Si shell. We consider a range of Si shell thicknesses, $t = (b - a)$ ranging from 0 to infinity, and evaluate the critical radius as a function of Ge nanocrystallite radius and Si shell thickness.

The total elastic strain energy is the elastic strain energy stored both in the germanium nanocrystallite and the Si shell, which can be computed from the stress and strain fields.

The system possesses spherical symmetry and the displacements and fields are only a function of the radial coordinate r. The misfitting Ge nanocrystallite produces a tensile stress on the interface, while the outer surface of the Si shell is traction free.

The stress and strain fields inside the spherical germanium nanocrystallite are purely hydrostatic. The hydrostatic stress component is the interface pressure, p, between the Ge nanocrystallite and the Si shell.

$$\sigma_{rr}^{Ge} = \sigma_{\theta\theta}^{Ge} = \sigma_{\phi\phi}^{Ge} = -p \tag{2.3}$$

For a stress free outer boundary this interface pressure is given by [22]

$$p = \frac{\frac{2E_{Si}}{3(1-\nu_{Si})}\epsilon\,(1-c)}{1-\frac{2m}{3}\,(1-c)} \tag{2.4}$$

where, E_{Si} is the Young's modulus of Si, ν_{Si} is the Poison's ratio of Si,

$c = \frac{a^3}{b^3}$ is the volume fraction of the nanocrystallite

$m = \frac{E_{Si}}{(1-\nu_{Si})}\left[\frac{(1-2\nu_{Si})}{E_{Si}} - \frac{(1-\nu_{Ge})}{E_{Ge}}\right]$ is the elastic mismatch parameter and

$\epsilon = \left(\frac{3K_{Ge}}{3K_{Ge}+4\mu_{Si}}\right)\left(\frac{a_{Ge}-a_{Si}}{a_{Si}}\right)$ is the constrained strain for a spherical geometry as defined by Eshelby [23] and Nabarro [14] , K_{Ge} is the Bulk modulus of Ge and μ_{Si} the shear modulus of Si. The constrained strain is calculated assuming that the lattice parameter of the nanocrystallite is the same as in bulk.

The stress and strain fields in the silicon shell vary according to the distance from the center of the nanocrystallite [24].

$$\sigma_{rrSi} = \frac{cp}{(1-c)}\left[1-\left(\frac{b}{r}\right)^3\right] \tag{2.5}$$

$$\sigma_{\theta\theta}^{Si} = \sigma_{\phi\phi}^{Si} = \frac{cp}{(1-c)}\left[1+\frac{1}{2}\left(\frac{b}{r}\right)^3\right] \tag{2.6}$$

The radial and tangential components of the strain fields (for a 50 Å A Ge nanocrystallite with a 950 Å thick Si shell) are shown in Figs. 2-2 and 2-3 respectively.

For the system considered, the elastic strain energy is,

$$E_{Elastic} = \frac{1}{2}\left(3\sigma_{rr}^{Ge}e_{rr}^{Ge}\right)\left(\frac{4}{3}\pi a^3\right) + \frac{1}{2}\int_b^a \left(\sigma_{rr}^{Si}e_{rr}^{Si} + 2\sigma_{\theta\theta}^{Si}e_{\theta\theta}^{Si}\right)\left(4\pi r^2 dr\right) \tag{2.7}$$

where the first term is due to the Ge nanocrystallite and the second term is due to the Si shell. Upon substitution of the relevant terms it simplifies to,

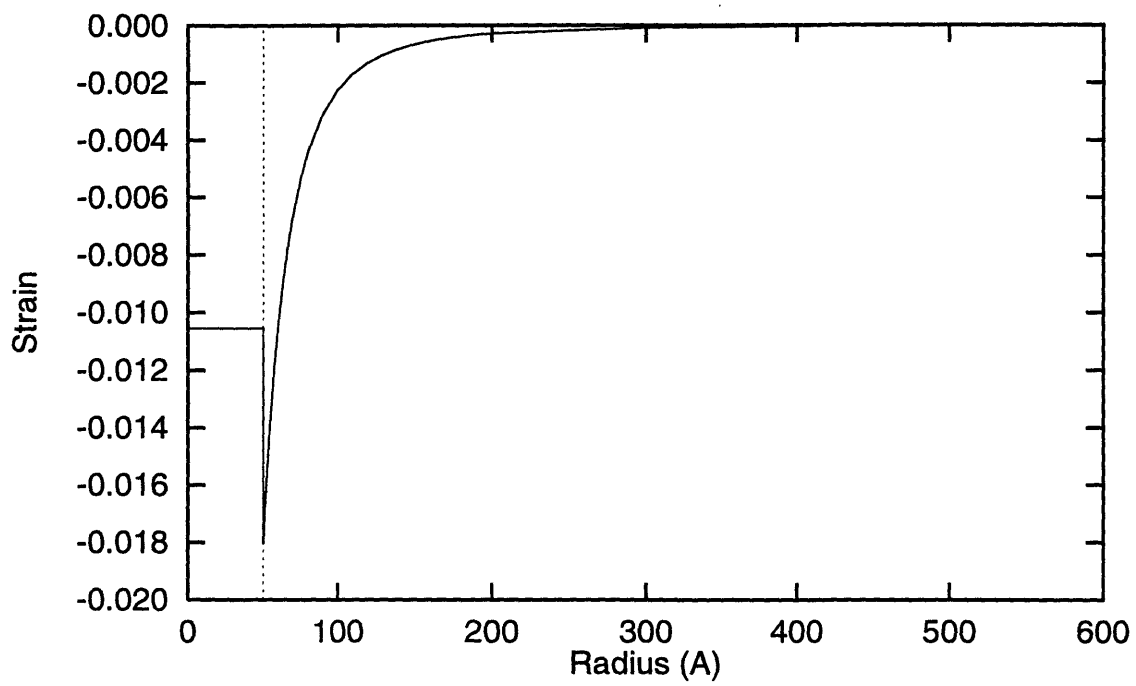

Figure 2-2: Radial strain field for a 50 Å Ge nanocrystallite with a 350 Å thick Si shell

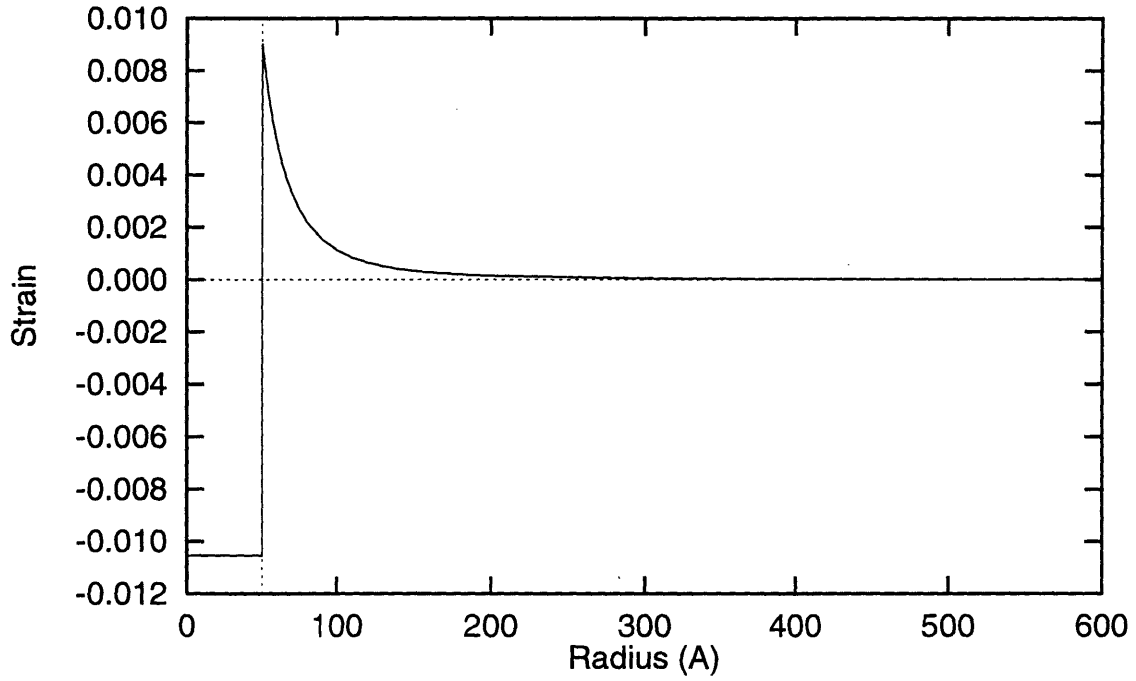

Figure 2-3: Tangential strain field for a 50 Å Ge nanocrystallite with a 350 Å thick Si shell

$$E_{Elastic} = \left(\pi a^3 p^2\right)\left[\frac{1-2\nu_{Ge}}{1+\nu_{Ge}}\frac{1}{\mu_{Ge}} + \frac{1-2\nu_{Si}}{1+\nu_{Si}}\frac{1}{\mu_{Si}}\frac{c}{(1-c)} + \frac{1}{2\mu_{Si}(1-c)}\right] \quad (2.8)$$

2.2.2 Incoherent State

The interface between the Ge nanocrystallite and the Si shell can become incoherent when the introduction of interfacial defects lowers the energy of the system.

Defect Energy

Our predictions of critical radius of the Ge nanocrystallite will depend on our judicious choice of the possible incoherency defects. We consider both strain relief by a perfect dislocation loop and by a stacking fault bounded by a partial dislocation loop. It is reasonable to assume that a dislocation loop is preferred over a set of dislocations that terminate at the surface.

To determine the dislocation energy we assume, that the energy required to create the dislocation loop in a finite medium is the same as the energy required to create the dislocation in an infinite medium. This assumption is valid until the shell thickness becomes so small that the dislocation interacts with the free surface.

The energy to create a circular dislocation loop in an infinite medium, with Burgers vector perpendicular to the plane of the loop is calculated by approximating the true dislocation configuration by piece wise straight configurations. Each segment of the loop is acted upon by a force caused by the stress originating from all other parts of the loop, and the work done against all these forces is the work done to create the dislocation loop. Thus, the interaction energy between all segments of loop (approximated into a piece wise-straight configuration) can be calculated accurately as [25]:

$$E_{Loop} = 2\pi r_{loop}\left(\frac{\mu|b|^2}{4\pi(1-\nu)}\right) ln\left(\frac{8\alpha r_{loop}}{|b|} - 1\right) \quad (2.9)$$

where, α is the dislocation core parameter, r_{loop} is the radius of the dislocation loop

and $|b|$ is the burgers vector of the dislocation loop.

Perfect Dislocation loops: We assume the dislocations to be vacancy type prismatic dislocation loops with burgers vector $\left(|b| = \frac{1}{2} < 110 >\right)$ perpendicular to the plane of the loop. The dislocation loop is assumed to be at the interface between the Ge nanocrystallite and the Si shell. Further, the radius of the dislocation loop is assumed to be the radius of the Ge nanocrystallite.

As the dislocation loop is created at the interface between the Ge nanocrystallite and the Si shell, we use the average shear modulus of the interface [26] $\mu_{interface} = \frac{2\mu_{Si}\mu_{Ge}}{(\mu_{Si}+\mu_{Ge})}$ in equation 2.9.

The defect energy in equation 2.2 for this defect is the energy of the dislocation loop.

Partial dislocations enclosing a stacking fault: An alternate mechanism for strain relief is assumed to be by a Frank partial dislocation loop with burgers vector $\left(|b| = \frac{1}{3} < 111 >\right)$ bounding an intrinsic stacking fault. The energy required to create this partial loop is given by equation 2.9, and the energy to create the intrinsic stacking fault is

$$E_{Stacking\ Fault} = \pi r_{loop}^2 \gamma \tag{2.10}$$

where, γ is the stacking fault energy of Ge. The defect energy in equation 2.2 for this defect is,

$$E_{Defect} = E_{Loop} + E_{Stacking\ Fault} \tag{2.11}$$

Residual Elastic Energy

The stress field of the dislocation relieves part of the strain in the misfitting system. The energy released by loop formation (interaction energy) is evaluated without using explicit expressions for the field of the dislocation, following the general procedure outlined by Eshelby [23].

$$E_{Interaction} = \pi r_{loop}^2 p|b| \tag{2.12}$$

where, r_{loop} is the radius of the dislocation loop formed at the interface between the Ge nanocrystallite and the Si shell, p the interface pressure as defined in equation 2.9 and $|b|$ is the Burgers vector of the loop formed. In the case of partial dislocation enclosing a stacking fault, there is no strain relief by the stacking fault and all the strain relief is by the partial dislocation.

The contribution of this strain relieving mechanism to the residual elastic energy of the system can be considered by subtracting the interaction energy from the elastic energy.

$$E_{Residual\ Elastic} = E_{Elastic} - E_{Interaction} \tag{2.13}$$

2.3 Results and Discussion

In calculating the energies of the states to estimate the critical radius, we use the following values for the parameters: $\mu_{Si} = 66.6\ GPa$, $E_{Si} = 162.9\ GPa$, $\nu_{Si} = .22$, $\mu_{Ge} = 54.6\ GPa$, $E_{Ge} = 132.8\ GPa$, $\nu_{Ge} = .21$[27], $\gamma_{Ge} = 60\ mJ/m^2$[28], $\alpha = 4$[29].

Fig. 2-4, shows the critical radius of the Ge nanocrystallite as a function of the Si shell thickness. We find that, for very thick Si shells ($> 1000\mathring{A}$), the Ge-Si interface remains coherent up to a Ge nanocrystallite radius of 100 Å. The critical radius of the Ge nanocrystallite in a very thick shell is found to be approximately three times the critical thickness of a Ge film on an infinite Si substrate. This can be explained in terms of the interface area to volume ratio. For a given volume of Ge nanocrystallite or film, the interface area between the spherical nanocrystallite and the Si matrix is less than the interface area between the Ge film and Si substrate. Therefore, the strain relief provided by introducing dislocations for the Ge nanocrystallite is smaller than for the Ge film of the equal volume. Hence generating dislocations in a nanocrystallite becomes less favorable until much larger radii.

For a thinner Si shell, the critical radius of the Ge nanocrystallite increases significantly as the total strain energy of the system decreases. As the Ge nanocrystallite radius increases, it becomes energetically less favorable to create partial dislocations enclosing stacking faults at a Ge nanocrystallite radius of greater than 270 Å. There-

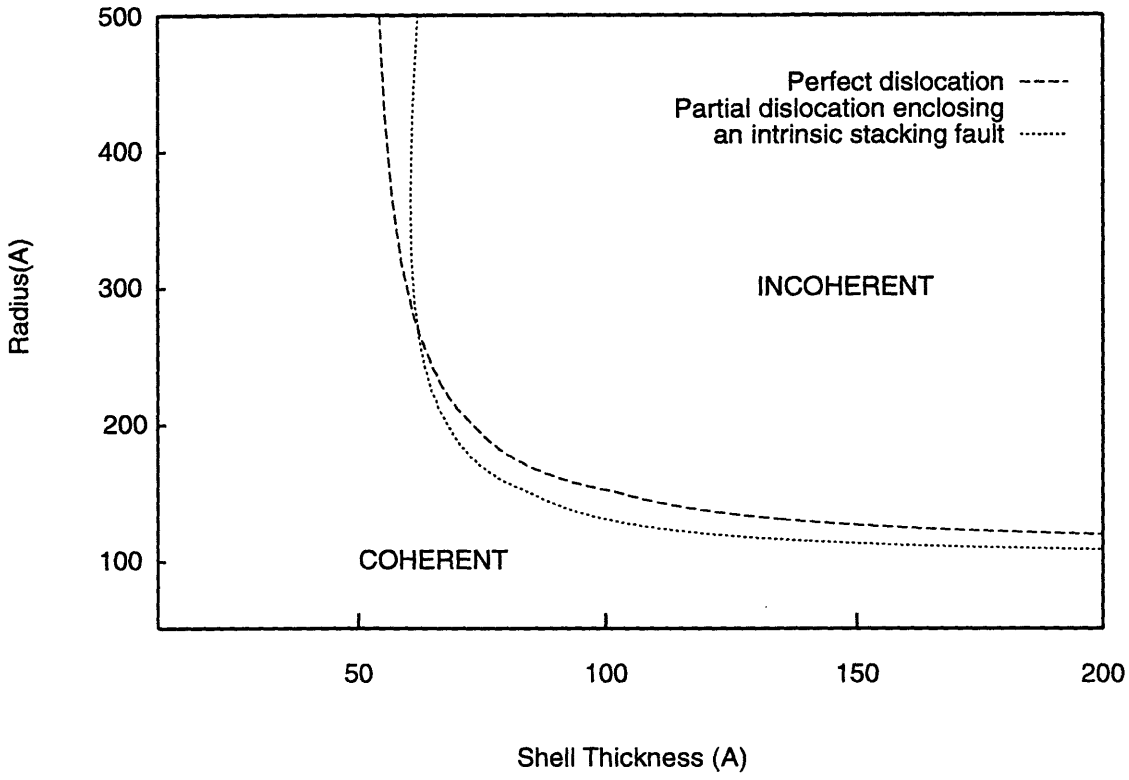

Figure 2-4: Contour of critical radius as a function of Si shell thickness and Ge nanocrystallite radius

fore, coherency is lost by forming a perfect dislocation loop rather than creating a partial dislocation loop enclosing a stacking fault.

We now asses the validity of the approximations made in our calculations. At very small shell thicknesses, the energy required to create the dislocation in a finite medium is not equal to that in an infinite medium. The effect of the free surface on the dislocation loop has to be considered in evaluating the energy required to generate the dislocation. This interaction between the dislocation and the free surface decreases the energy of the system in the incoherent state, hence the critical radius for systems with very small shell thickness will be lower than what we have estimated.

The values used for the parameters in these calculations are approximate. We tested the sensitivity of our results on the value used for the parameters.

In evaluating the energy required to create a dislocation loop (perfect or partial) we use a dislocation core parameter, α, of 4 [29], which is typical for diamond cubic

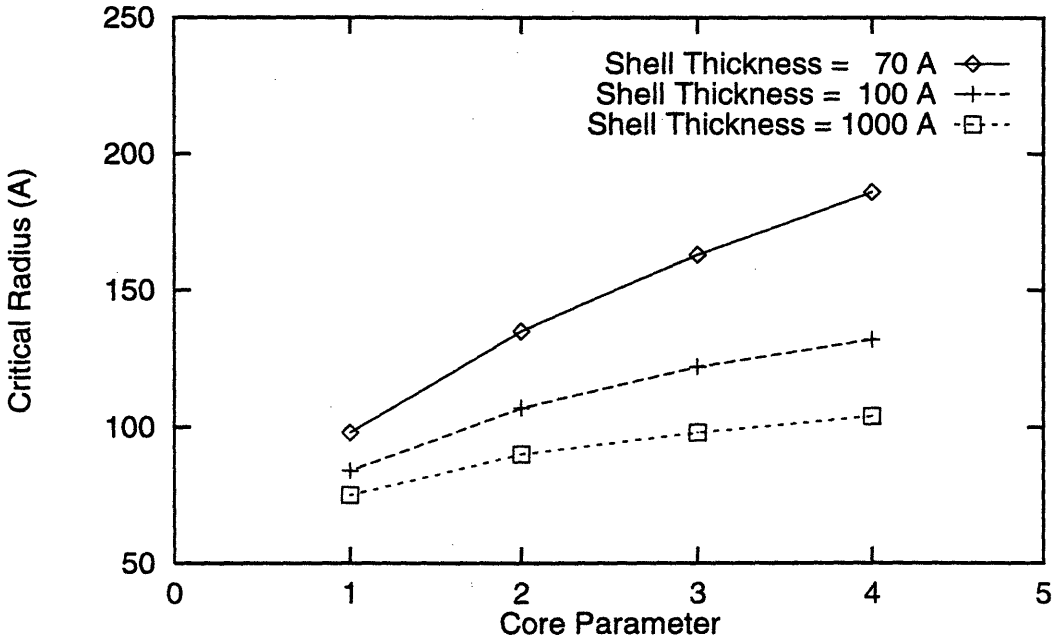

Figure 2-5: Variation of the critical radius of Germanium as a function of the core radius of the partial dislocations considered (assuming partials and stacking faults cause the loss of coherency)

materials. However, other values ranging between 1 and 5 have been used in the literature. Therefore the critical radius is also evaluated as a function of dislocation core parameter at various shell thicknesses, as shown in Fig.2-5. The critical radius is found to vary substantially with the core parameter α. The effect of dislocation core parameter on the critical radius is more pronounced at smaller Si shell thicknesses.

In evaluating the energy required to create an intrinsic stacking fault, we use a Ge stacking fault energy of 60 mJ/m^2. However, there remains some disagreement in measurements of stacking fault energies in Ge. Intrinsic stacking fault energies of 30 mJ/m^2 [30] and 60 mJ/m^2 [28] have been reported in literature. The critical radius is evaluated as a function of stacking fault energy at various shell thicknesses, as shown in Fig.2-6. The critical radius is found to increase as the stacking fault energy increases. The effect of stacking fault energy on the critical radius is more pronounced at smaller Si shell thicknesses.

The interaction energy (energy released by loop formation) can at most be equal

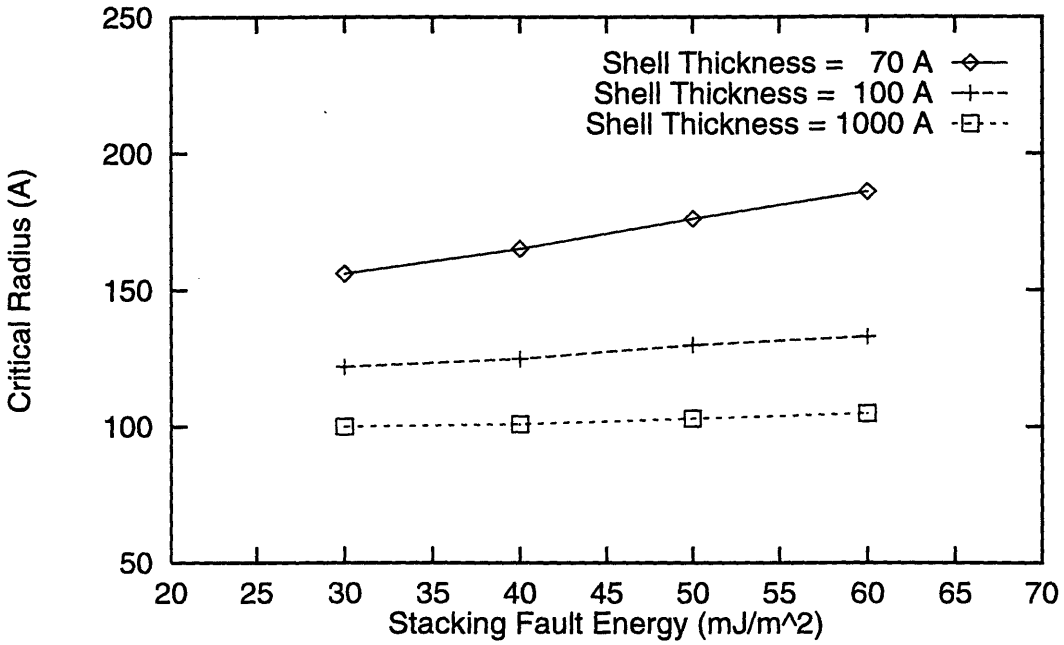

Figure 2-6: Effect of Stacking fault energy on the critical radius

to the elastic strain energy of the system. In our model, this condition is satisfied only for Ge nanocrystallites with radii greater than 20 Å, limiting the applicability of this method.

2.4 Conclusions

The system is coherent up to a Ge nanocrystallite radius of about 100 Å, irrespective of the Si shell thickness. Nanocrystallites of radii larger than 270 Å lose coherency by the generation of perfect dislocation loops. For intermediate Ge nanocrystallite radii (between 100 Å and 270 Å) . the coherency is lost by the introduction of partial dislocation loops enclosing a stacking fault. As the shell thickness decreases, the critical radius increases.

The significant effect of the stacking fault energy and dislocation core parameter on the critical radius is found to be more significant at smaller shell thicknesses, indicating the approximate nature of these calculations. Typical nanocrystallite radii

of experimental interest are of the order of 50 Å or less. Therefore, we conclude that extremely large Ge nanocrystallites capped with Si shells can be grown without producing dislocations. We view this as an important determination in our efforts to experimentally grow these structures.

Chapter 3

Effect of atomic environment and strain on the activation energy for inter-diffusion of Ge in Si

3.1 Introduction

Electrical properties of nanocrystallites depend critically on the "perfection" of the interface between the nanocrystallite and the host. Imperfections around the interface can arise from lattice imperfections (misfit dislocations) or from interdiffusion of atoms between the nanocrystallite and the host. Coherency loss by the generation of lattice imperfections has been investigated in Chapter 2. In this chapter, we study the interdiffusion of atoms between the nanocrystallite and the host.

Interdiffusion is observed experimentally at temperatures above 1000° C, in one-dimensional Si/Ge quantum well heterostructures [31, 32]. However, unlike quantum wells, the interface between the nanocrystallite and the host has all crystallographic planes. This makes interdiffusion more complex to study in quantum dot systems.

From a purely thermodynamical standpoint, at 1000° C, Si and Ge form a continuous solid solution (Fig. 3-1). Therefore, at equilibrium, we would expect the Ge-Si interface to be completely intermixed. However, the thermodynamic driving force

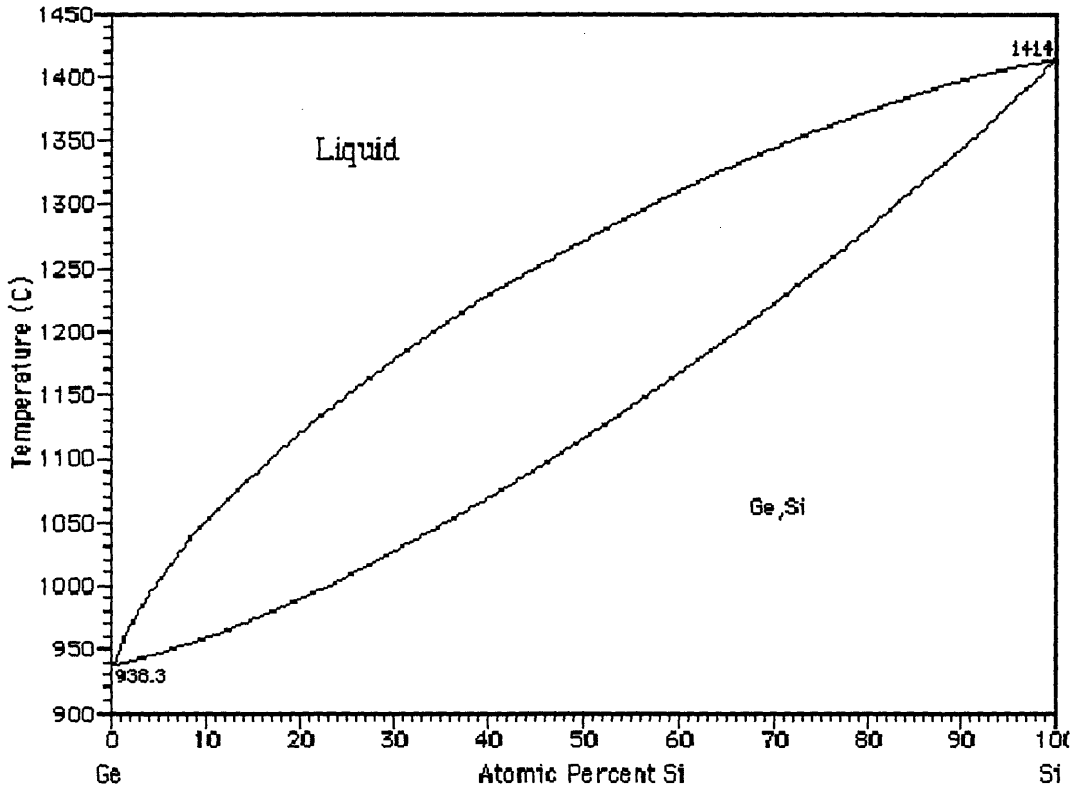

Figure 3-1: Si-Ge Phase diagram showing a continuous solid solution at high temperatures.

alone will not determine how quickly this equilibrium will be reached and kinetic factors have to be taken into account.

When interdiffusion occurs, the atoms to be exchanged go from the initial state to the final state through an activated state. The activated state corresponds to the state with maximum energy (activation energy) on the minimum energy path for diffusion. Depending on the thermal energy available, the system may or may not overcome this activation energy barrier. Therefore, as a first step towards understanding the interdiffusion path at short times, we computed the activation energy for the interdiffusion of Ge and Si in the nanocrystallite/host system. The activation energy depends on the diffusion mechanism (the exact path to exchange), strain, and the atomic environment (local and long range). In this thesis, we study the effect of these parameters on the activation energy.

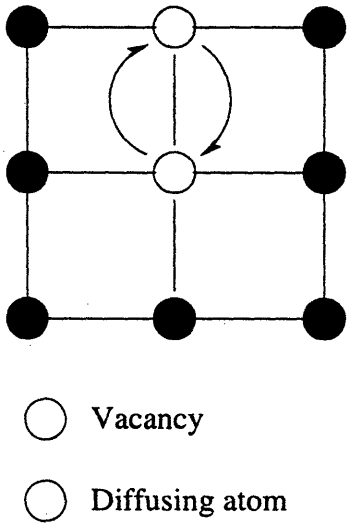

Figure 3-2: Vacancy Mechanism: The diffusing atom moves down by one nearest-neighbor distance on the regular lattice of atoms. This is accomplished by jumping into the vacancy below it.

There is considerable disagreement on the diffusion mechanism in Si and in Ge. Therefore, before calculating the activation energy we need to establish the diffusion mechanism taking place. This will be discussed in the next section.

3.2 Diffusion mechanisms

Self Diffusion in bulk crystalline Silicon and Germanium:

Diffusion may occur through an *indirect mechanism* (vacancy or interstitialcy mechanism) or through a *direct mechanism* (nearest-neighbor exchange, ring, or concerted exchange mechanism) [33].

The indirect diffusion mechanism requires intrinsic defects such as vacancies or interstitials for facilitating the diffusion process.

The *Vacancy mechanism* involves the diffusion of the diffusing atom into the vacancy site and a consequent movement of the vacancy in the opposite direction (Fig. 3-2). It is argued that this mechanism controls the diffusion in Ge at all temperatures and in Si at temperatures below 1000° C [33].

The *Interstitialcy mechanism* involves the diffusion of a self interstitial (Fig. 3-

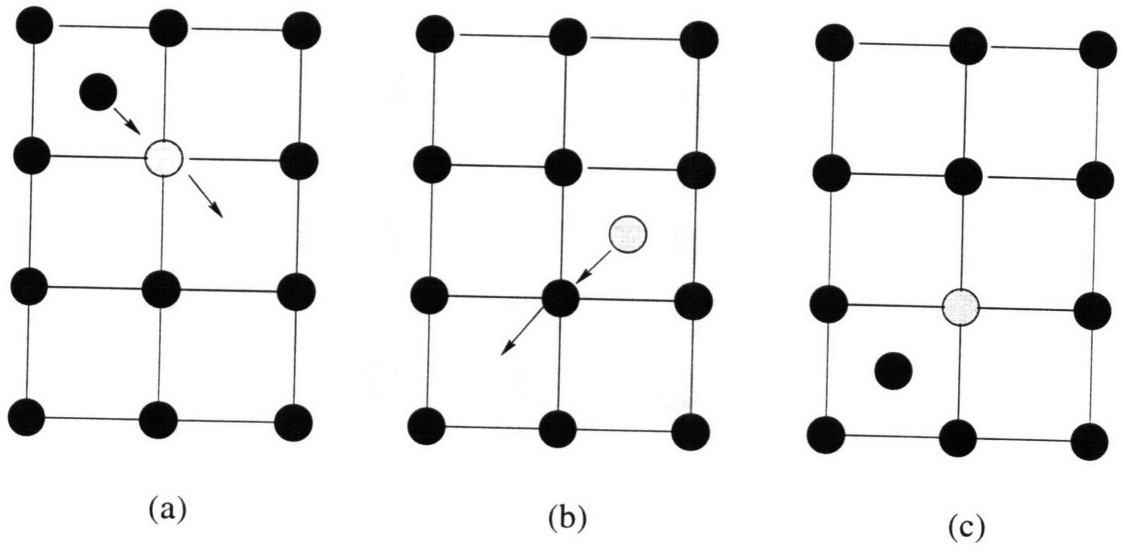

Figure 3-3: Interstitialcy mechanism: In (a) the self interstitial has approached the diffusing atom; in (b) the diffusing atom has been temporarily displaced to an interstitial site while the original self interstitial has occupied a regular lattice site. In (c) the diffusing atom has re-occupied a regular lattice site by kicking a self atom into an interstitial site.

3a) into the site of the diffusing atom by displacing it to another interstitial site. The diffusing atom is temporarily at the interstitial site (Fig. 3-3b) until it displaces a neighboring atom into another interstitial site and occupies a regular lattice site (Fig. 3-3c). It is argued that this mechanism controls the self-diffusion in Si above 1000° C [33].

By contrast, the direct mechanisms do not require the generation of any defects like vacancies or self interstitials. The diffusing atom diffuses in an otherwise perfect lattice through a direct exchange of two atoms on neighboring sites. This can occur in a single step as in the direct exchange (Fig. 3-4) and ring mechanisms (Fig. 3-5) or through a sequence of steps as in the concerted exchange mechanism.

The single step exchange processes occur by the rotation of the two atoms about their common center of of separation. This involves considerable distortion of the surrounding structure. Therefore, they are energetically unfavorable compared to the indirect mechanisms.

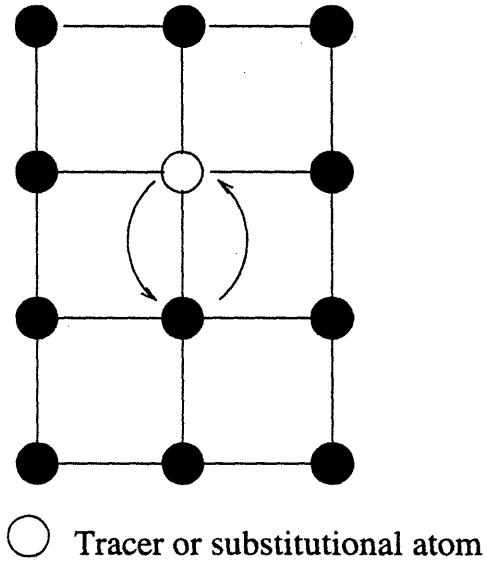

Figure 3-4: Single step direct exchange mechanism of two atoms on neighboring sites.

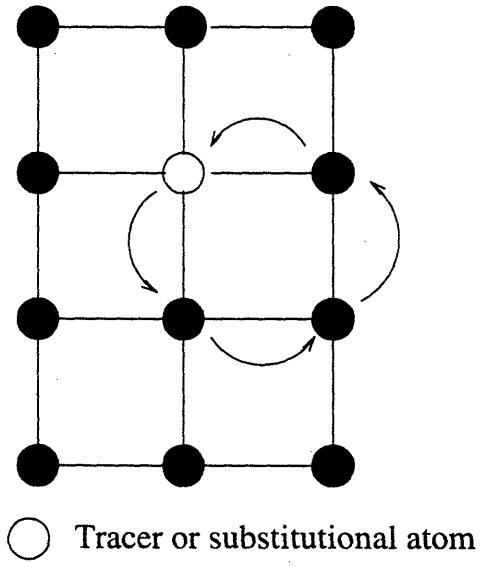

Figure 3-5: Ring mechanism

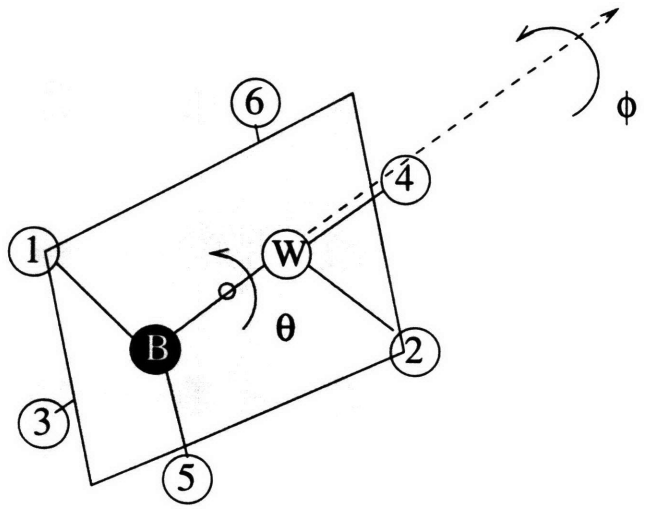

Figure 3-6: Concerted exchange mechanism. The Black atom (B) and the White atom (W) are the atoms to be exchanged. Atoms 1 through 6 are the first neighbor atoms.

The *Concerted Exchange (CE) mechanism* – (proposed for the diffusion of substitutional atoms in Si [34]) on the other hand, takes place through a set of intermediate steps such that, at every step, the distortion and the number of broken bonds are kept to a minimum. In this process, bonds attached to the atoms to be exchanged are broken and formed in succession such that at every stage, no more than two bonds are broken. In Fig. 3-6, the black atom (B) and the white atom (W) are the atoms to be exchanged, and atoms 1 through 6 are the first neighbor atoms. The grey plane contains the atoms to be exchanged (B and W)) and a pair of neighboring atoms (atoms 1 and 2) attached to them. The CE mechanism can be described in terms of two independent rotations of B and W (Fig. 3-6). The first is a rotation of B and W by an angle θ about an axis passing through the center of the bond between them. perpendicular to the grey plane shown in Fig. 3-6. The second is a rot ation of B and W by an angle ϕ about the original bond between them (direction shown with dotted lines in Fig. 3-6).

In the concerted exchange process, the activated state (saddle point) on the unique

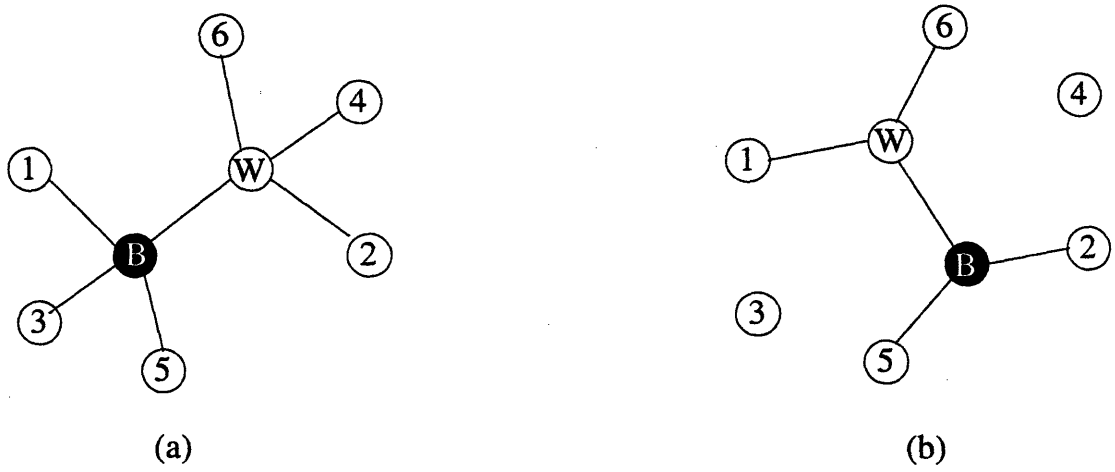

Figure 3-7: In (a) Initial state of the system (b) Activated state of the system : The Black atom (B) and the White atom (W) are the atoms to be exchanged. Atoms 1 through 6 are the first neighbor atoms. In the activated state two bonds B-3 and W-4 are broken

low energy path to exchange is clearly defined. In reaching the activated state shown in Fig. 3-7(b), the atoms to be exchanged were rotated (sense of rotation shown in Fig. 3-6) such that bonds B-1 (between the black atom and atom 1) and W-2 (between the white atom and atom 2) were first broken. This was followed by a rotation such that bonds W-1 and B-2 were formed, thereby completing part of the exchange. This was followed by a rotation such that atoms B-3 and W-4 were broken. This corresponds to the activated state and can be obtained from the initial state by a rotation of $\theta = 90°$ and $\phi = 30°$. In this process, bonds B-5 and W-6 have not been broken. Therefore we refer to this plane (5-B-W-6) containing atoms 5 and 6 (the nearest neighbor atoms to B and W) which have not been affected in reaching the activated state as the *unaffected plane*. Similarly, the activated state can be reached by having neighboring atoms 1 and 2 on the unaffected plane (plane 1-B-W-2) or neighboring atoms 3 and 4 on the unaffected plane (plane 3-B-W-4).

The activation energy for self diffusion of Si predicted by the CE mechanism is lower than or comparable to the activation energies computed for the vacancy and interstitialcy mechanisms [34]. Therefore, the concerted exchange mechanism is a

possible mechanism for self diffusion of Si. It is assumed to be the preferred diffusion mechanism because it can qualitatively explain the experimental observations [33] (large entropy for Si self-diffusion, slower diffusivity of Group IV elements in Si than group V elements, non-Arrhenius nature of diffusion) which cannot be explained by the vacancy or interstitialcy mechanism.

For the purpose of this study, we assumed that the material is initially free of defects and that diffusion is by concerted exchange. It must be noted that, in the presence of vacancies or interstitials in the material, these defect mechanisms may compete.

To calculate the activation energy it is important to choose an energy model. Energy models can be based on ab-initio calculations or empirical potentials. Ab-initio calculations are accurate but very time consuming while energy models based on empirical potentials are fast but approximate. In this study we used empirical potentials models to calculate the activation energy.

3.3 Empirical Potentials

There are many published potentials for Si and Ge [35, 36, 37, 38, 39, 40]. These, empirical potentials best reproduce the properties they have been fitted to and may not be reliable for reproducing other properties. For example, Pandey computed the total-energy surface for self-diffusion of Si by the CE mechanism from first principles [34]. This calculation showed that the activated state corresponded to a saddle point on the minimum energy path for diffusion. However, as shown by Kaxiras [41], some potentials like the Tersoff [39, 40] and Dodson [42] potentials predict a local-minimum in energy corresponding to the activated state configuration.

The Kaxiras-Pandey potential [41] reproduces the energy surface for the concerted exchange mechanism in Si with high accuracy. However, potentials with similar qualities for Ge and the Si-Ge system are not available. In this study, we developed a potential that qualitatively describes the activated state and predicts the effect of environment and strain on the activation energy for diffusion by the concerted exchange

process.

The potential-energy function describing interactions between n particles can be resolved into one, two, three to n-body contributions:

$$V(1,...,n) = \sum_i V_1(i) + \sum_{i<j} V_2(i,j) + \sum_{i<j<k} V_3(i,j,k) + ... \tag{3.1}$$

The one-body potential is zero as there are no external forces acting on the system. We chose the two-body potential as a Lennard-Jones pair potential:

$$V_2(i,j) = \frac{A}{r_{ij}^{12}} - \frac{B}{r_{ij}^{6}} \tag{3.2}$$

where A and B are constants and r_{ij} is the interatomic distance. We use a cutoff distance of 2.7 Å, which takes into account the interaction between first nearest neighbor atoms. This potential alone will not stabilize a low coordination structure like the diamond cubic. Therefore, we also use a harmonic three-body potential that minimizes the energy of the crystal at the ideal diamond cubic bond angle of 109.47° (consequently stabilizing the diamond cubic structure). For every triad of atoms about atom i (Fig. 3-8), the three-body potential contributes to the total energy by an amount given by:

$$V_3(i,j,k) = 0.5 * K(\alpha_{jik} - \alpha_o)^2 \tag{3.3}$$

where, K is force constant between two atoms and α_o the the equilibrium angle about atom i. We selected cutoffs in the potentials which determine the range of interaction between atoms as given in Table 3.2.

We fitted the potential to the experimental elastic constants of Si and Ge [43] and elastic constants of Si-Ge in Zinc Blende structure calculated from first principle calculations[44]. The potential was also fitted to the equations of state (energy as a function of volume) obtained from first principle pseudopotential calculations for Si, Ge, and Si-Ge in the Zinc Blende structure [45]. The resulting parameters for the two- and three-body potentials are given in Table 3.1 and Table 3.2 respectively.

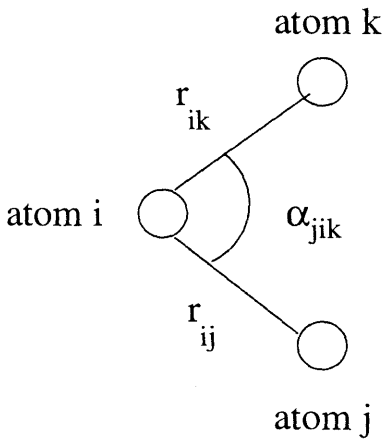

Figure 3-8: Triad of atoms

Table 3.1: Two-body potential

atom i	atom j	A (eV Å^{12})	B (eV Å^{6})	r_{12} (Å)
Ge	Ge	18586.67	193.13	2.7
Si	Si	20535.47	264.35	2.7
Si	Ge	20030.33	231.69	2.7

Table 3.2: Three-body potential

atom i	atom j	atom k	K (eV rad^{-2})	α_o (deg)	r_{12} (Å)	cutoff r_{13} (Å)	r_{23} (Å)
Ge	Ge	Ge	2.917	109.47	2.7	2.7	5.0
Si	Si	Si	2.828	109.47	2.7	2.7	5.0
Ge	Si	Si	2.924	109.47	2.7	2.7	5.0
Si	Ge	Ge	2.924	109.47	2.7	2.7	5.0
Si	Ge	Si	2.876	109.47	2.7	2.7	5.0
Ge	Si	Ge	2.921	109.47	2.7	2.7	5.0

3.3.1 Validity of potential

To test the applicability of the potentials, we computed the energy for Si self-diffusion over the concerted exchange path. The calculations were performed with GULP [46] - a general utility lattice program which performs energy minimizations, transition state calculations and defect calculations using an empirical potential model. The energies were calculated for the ideal CE path where the atoms to be exchanged are at their equilibrium separation. The total-energy along the ideal CE path as predicted by this potential is compared to the quantum-mechanical Local-Density-Functional (LDF) calculations of Pandey [34] (Fig. 3-9). In agreement with the LDF calculations, the energy of the activated state (calculated with our potential) is a maximum. The total energy shows a large increase at approximately $\theta = 60°, \phi = 0°$ which can be attributed to the cutoffs used in the potential. The activation energy predicted by the potential is larger than the LDF result. This is to be expected because the potential model is an approximation and in obtaining the two and three-body parameters, we have not fitted the potential to the activation energy. But, this potential is suitable to study the *qualitative* effect of configuration and strain on the activation energy.

To assess the validity of the Si and Ge potentials, we computed the activation energies for self-diffusion in Si and Ge and compared them to the experimental results [33]. The energies were calculated using the potentials by relaxing 123 atoms around the exchanged atoms. This was found to be sufficient as relaxing an additional layer of atoms did not decrease the activation energy of the system by more than 0.005 eV (Fig. 3-10).

The experimental results on Si self diffusion are less consistent than those on Ge self-diffusion (Fig. 3-11). The reason for the large discrepancies is not clear since most of the recent experiments have been performed on extremely pure,dislocation free single crystal Si. However, as evident from Fig. 3-11, the activation energies follow the same trend as the corresponding experimental values [33]. The agreement will be improved if we take into account the effect of long range relaxations. Long range relaxations result in greater lowering of the activation energy in Ge because of

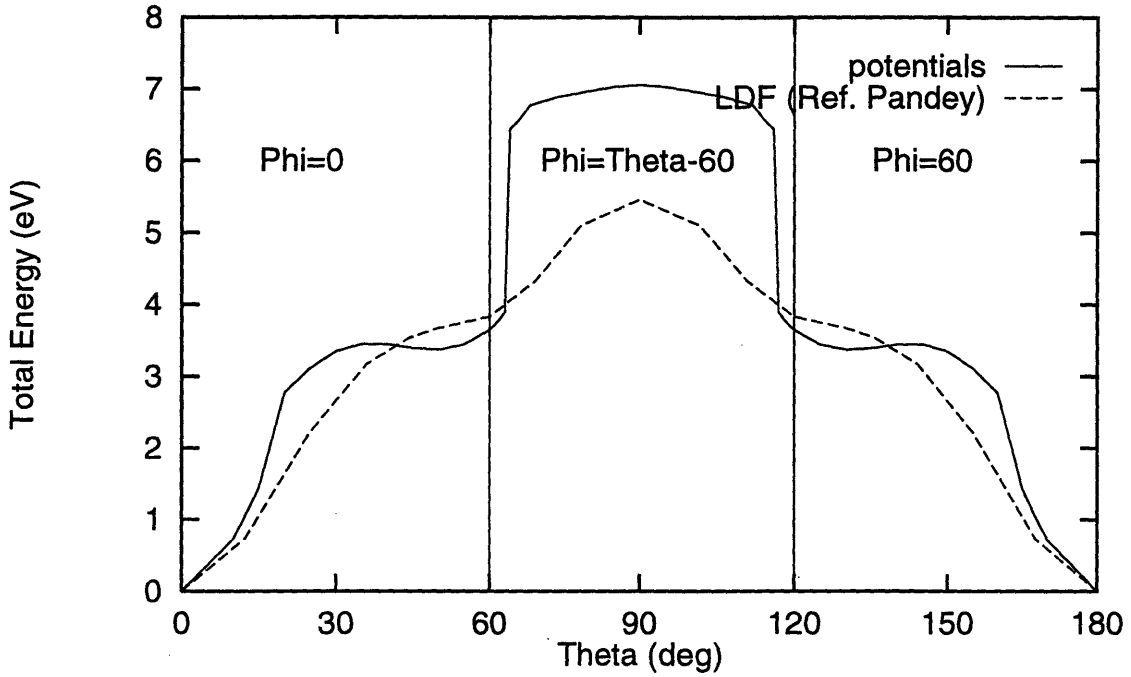

Figure 3-9: Total energy of ideal CE path for Si self diffusion as predicted by potentials

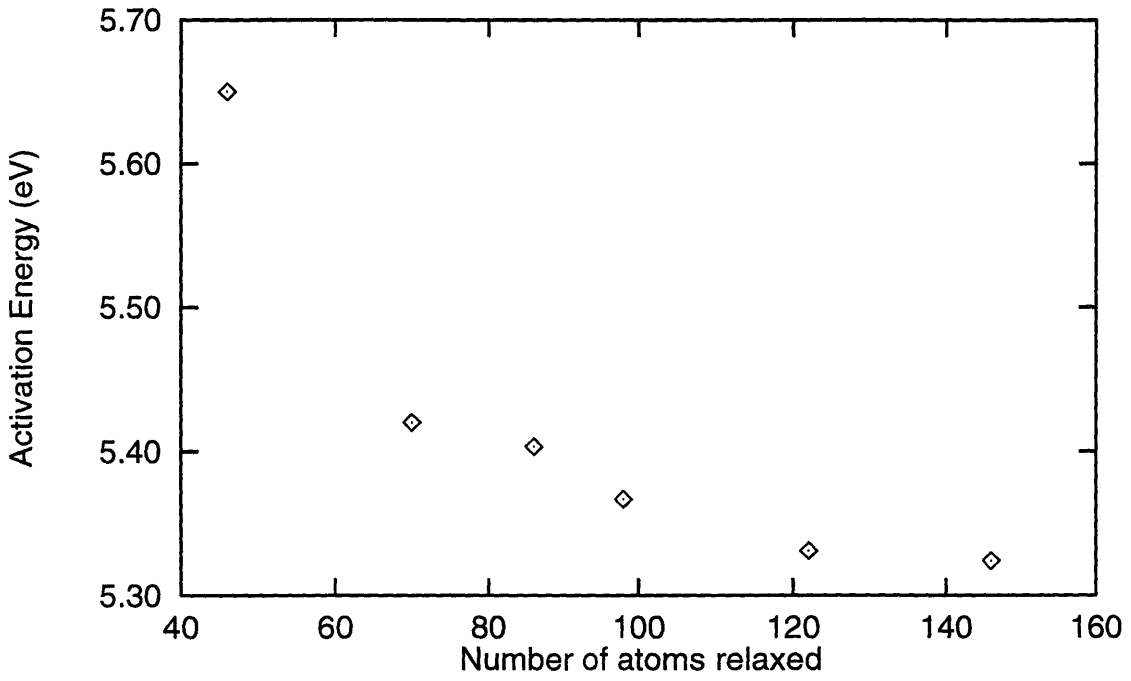

Figure 3-10: Activation energy as a function of number of atoms relaxed.

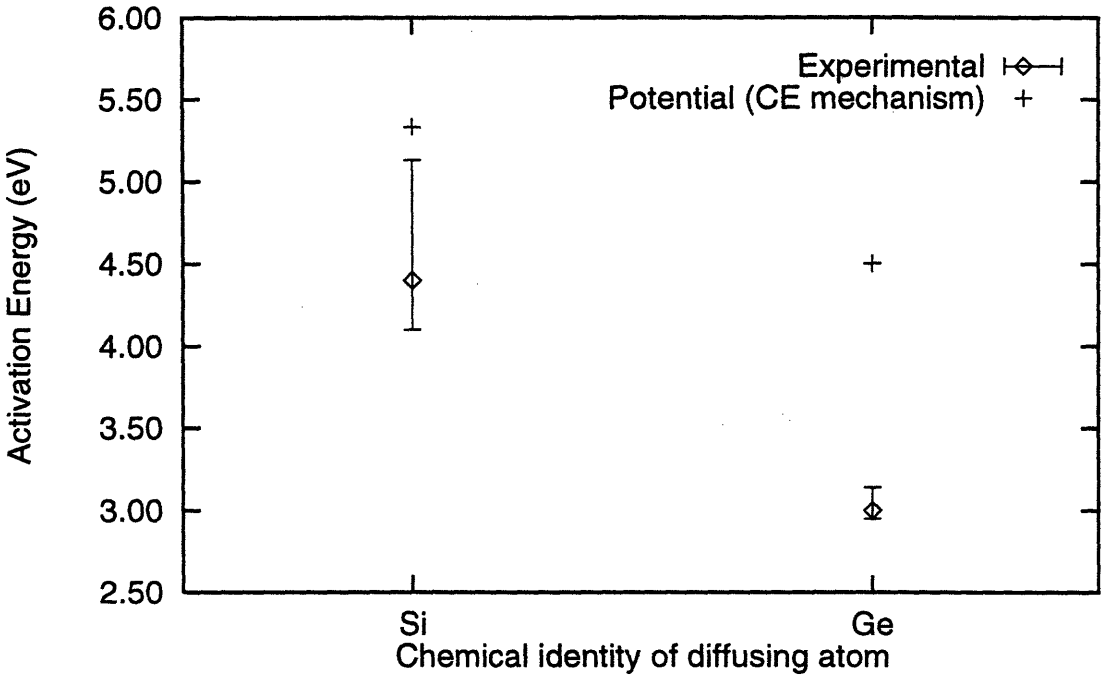

Figure 3-11: Activation Energy for self diffusion as predicted by potentials

its lower elastic modulus.

To asses the validity of the Si-Ge potential, we computed the formation energies of various ordered structures of Si and Ge using our potential and compared them to the pseudopotential calculation results of Qteish et.al. [47]. As shown in Fig. 3-12, our potential predicts the correct trend for the formation energies and hence their relative stabilities. Also, the lattice parameters predicted by our potential are within 0.8% of the lattice parameter predicted by Qteish et.al.. This gives us confidence in using our potential for predicting the qualitative trends in the activation energy for Si-Ge interdiffusion.

3.4 Results : Diffusion in bulk Si and Ge

3.4.1 Effect of neighbor atom identity on the activation energy

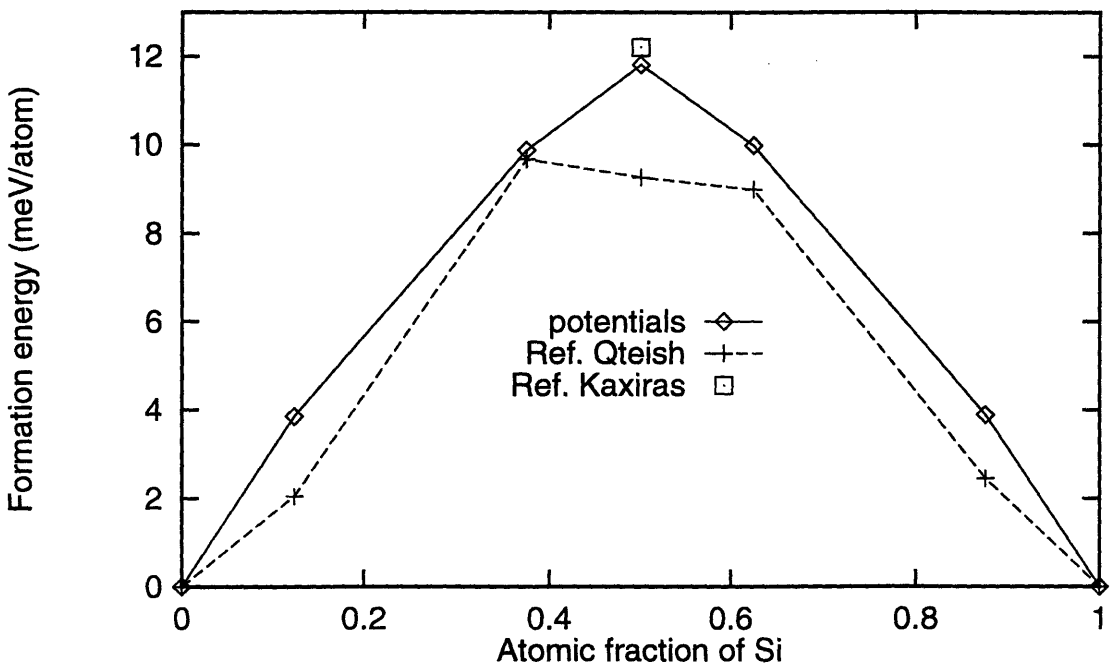

Figure 3-12: Formation energy vs. atomic fraction of Si as predicted by potentials

In this study, *first neighbors* are defined as all the nearest neighbors of the two atoms to be exchanged and *second neighbors* as the nearest neighbors of the first neighbors and so on. We computed the activation energy for the exchange of a Si-Ge pair in a pure Si matrix (E_{A0}). We then computed the activation energy (E_{Ai}) for the same exchange by changing the identity of one neighbor shell (i - first, second, or third neighbor) at a time from Si atoms to Ge atoms. The difference in activation energy ($E_{A0} - E_{Ai}$) corresponding to this change in i^{th} neighbor environment is plotted against the neighbor number in Fig. 3-13. We find that, going from first to second to third neighbor, the dependence of activation energy on the neighbor identity decreases (Fig. 3-13). The effect of the identity of third neighbors was found to be 0.01 eV. Therefore, we conclude that the activation energy can be calculated accurately (to within 0.01eV) by taking into account th e *identity* of the first and second neighbors.

3.4.2 First neighbors

We calculated the activation energy for the exchange of a Si-Ge pair in a pure

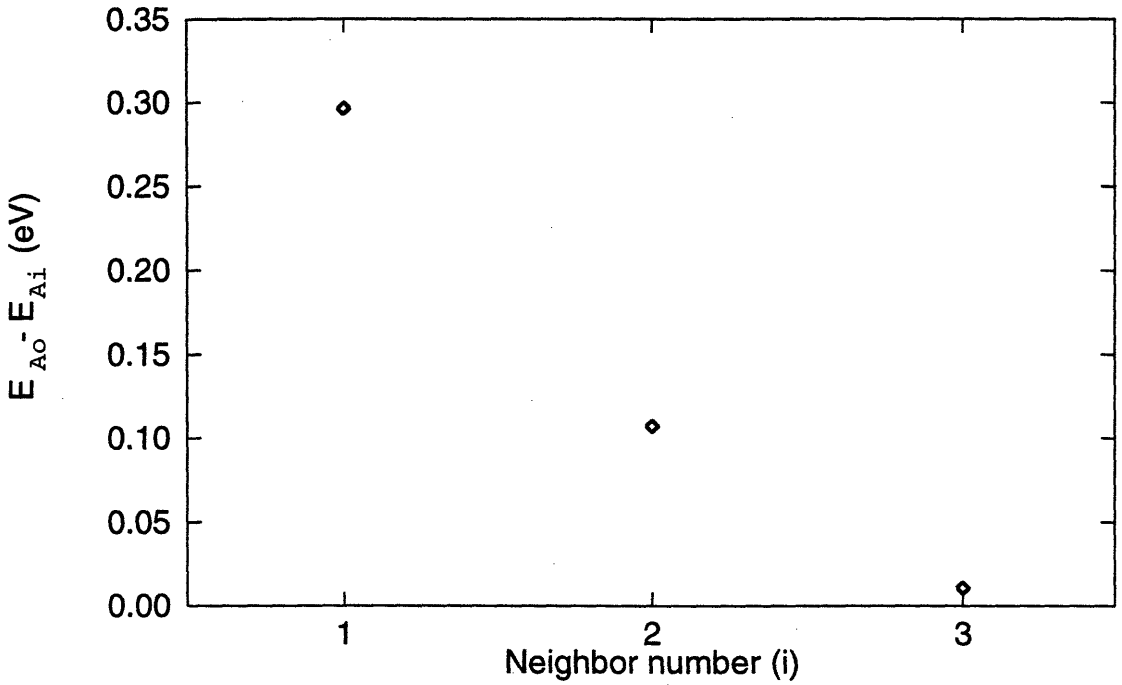

Figure 3-13: Effect of neighbor identity on activation energy. E_{A0} is the activation energy for the exchange of a Si-Ge pair in a pure Si matrix. E_{Ai} is the activation energy for the same exchange with one neighbor shell (i - first, second, or third neighbor) changed from Si atoms to Ge atoms

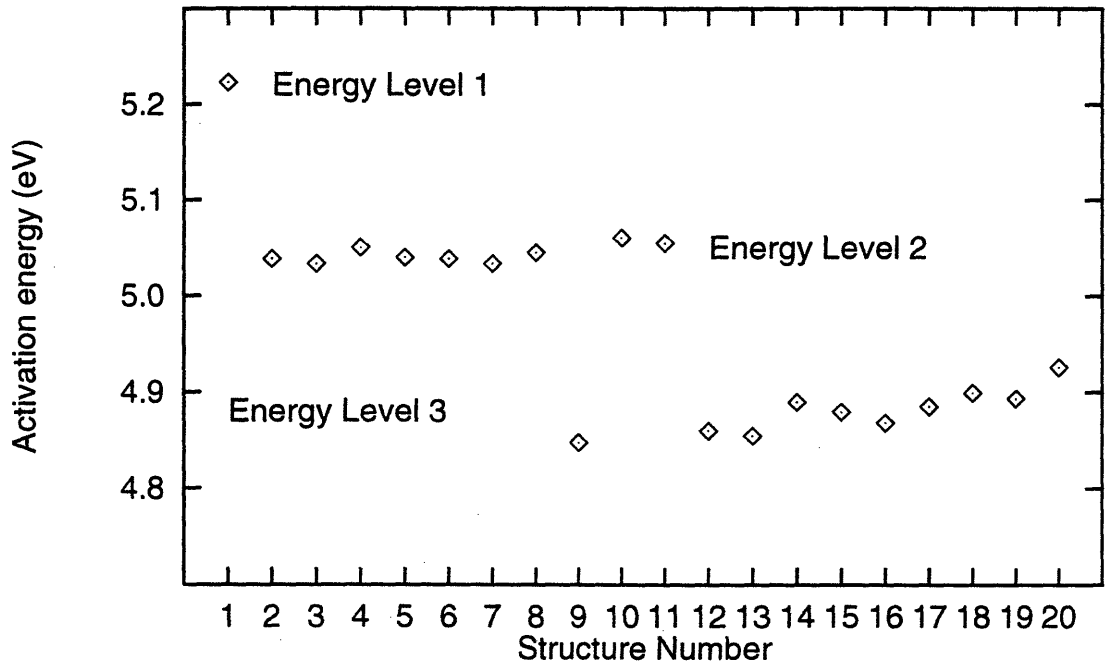

Figure 3-14: Effect of first neighbor environment on activation energy.

Si matrix with various first neighbor environments. We randomly assigned structure numbers to the 20 possible structures (shown in Fig. 3-15 and Fig. 3-16) with different first neighbor environments. The activation energy for the various structures was found to fall into three energy levels as shown in Fig. 3-14.

It was found that an activated state containing an unaffected plane with only Ge atoms attached to the atoms to be exchanged corresponds to the lowest energy - Energy Level 3 in Fig. 3-14. We refer to this plane as the *Ge-Ge unaffected plane.* An activated state containing no Ge-Ge unaffected plane but an unaffected plane with a Si atom and a Ge atom attached to the atoms to be exchanged corresponds to Energy Level 2 shown in Fig. 3-14. We refer to this plane as the *Si-Ge unaffected plane.* An activated state containing an unaffected plane with only Si atoms attached to the atoms to be exchanged corresponds to Energy Level 1 shown in Fig. 3-14. We refer to this plane as the *Si-Si unaffected plane.* This occurs when all first neighbor atoms are Si.

In reaching the activated state, the unaffected plane could be one of the three possible planes 1-B-W-2, 3-B-W-4, 5-B-W-6 in Fig. 3-7. The system chooses a plane with the lowest energy to be the unaffected plane. This is referred to as the "preferred unaffected plane". Depending on the first neighbor environment this could be a Ge-Ge or a Si-Ge or a Si-Si unaffected plane.

Consider structures 8 and 9 which have two Si atoms and one Ge atom attached to each atom to be exchanged (Fig. 3-14). Although they have the same number of first neighbors of a given chemical identity attached to the atoms to be exchanged, we find that the activation energies are in different levels. This is because the preferred unaffected plane is a Si-Ge unaffected plane in structure 8 but the preferred unaffected plane is a Ge-Ge unaffected plane in structure 9. A similar effect is seen in structures 10 and 12. Therefore, we conclude that the activation energy depends on the detailed arrangement of the atoms, i.e, the atoms on the preferred unaffected plane.

The other first neighbors (not on the preferred plane) have a much smaller impact on the activation energy. In Fig. 3-18, we plot the activation energy for various structures with the same preferred unaffected plane (Ge-Ge unaffected plane) but

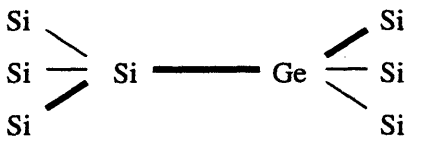

Structure 1

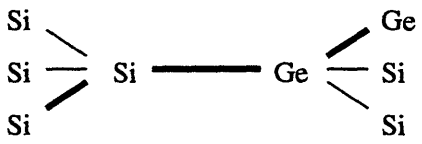

Structure 2

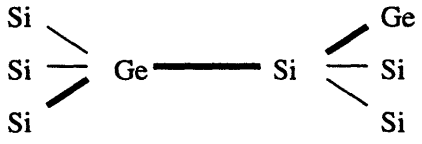

Structure 3

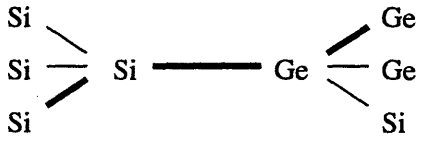

Structure 4

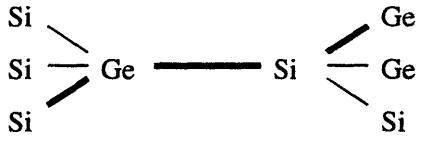

Structure 5

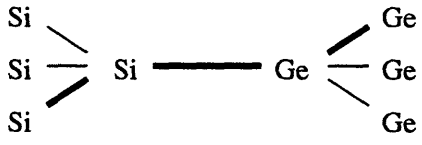

Structure 6

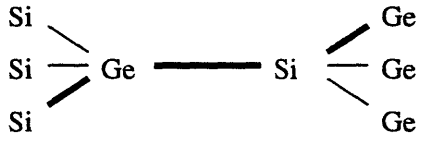

Structure 7

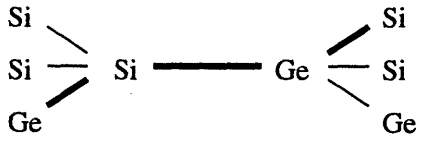

Structure 8

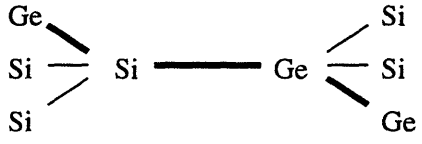

Structure 9

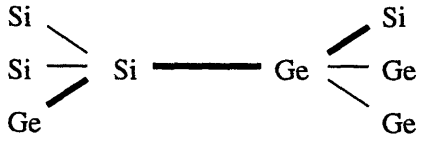

Structure 10

Figure 3-15: First neighbor environments. The plane containing the atoms to be exchanged attached to the first neighbors through bonds shown in bold corresponds to the *preferred unaffected plane* .

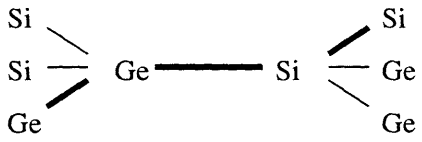

Structure 11

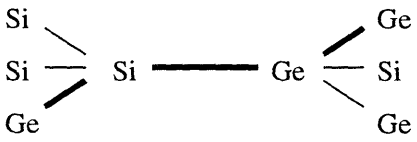

Structure 12

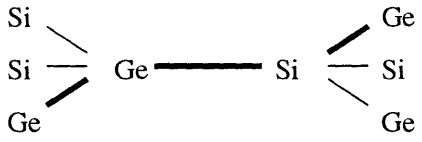

Structure 13

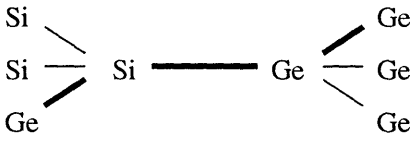

Structure 14

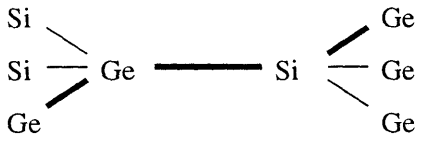

Structure 15

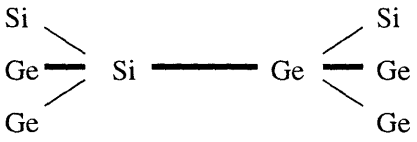

Structure 16

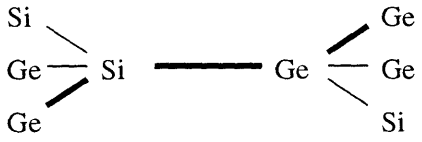

Structure 17

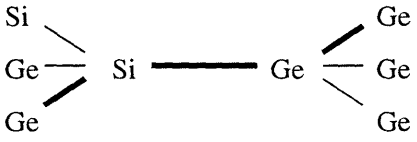

Structure 18

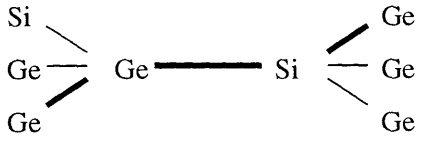

Structure 19

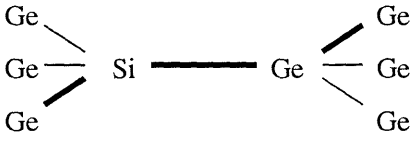

Structure 20

Figure 3-16: First neighbor environments. The plane containing the atoms to be exchanged attached to the first neighbors through bonds shown in bold corresponds to the *preferred unaffected plane* .

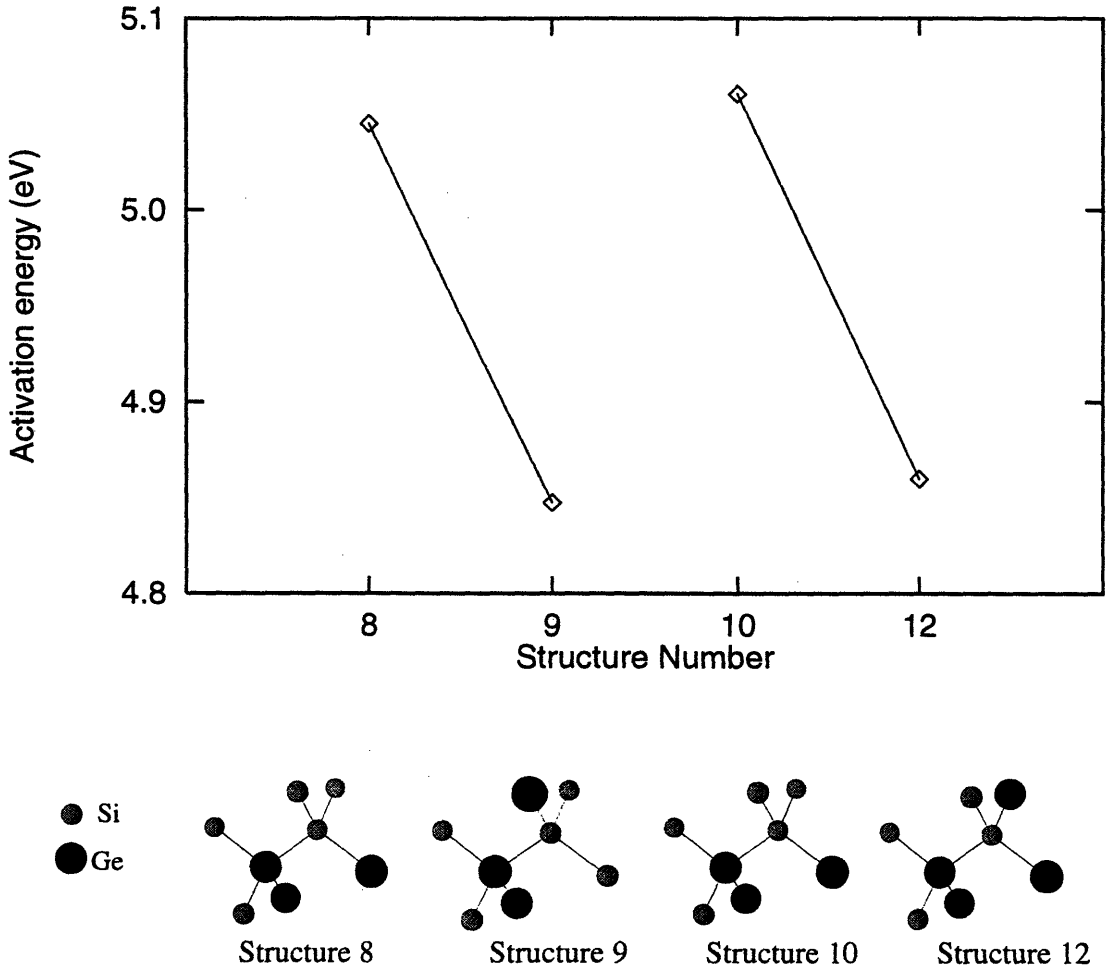

Figure 3-17: Specific examples for effect of atoms on the preferred unaffected plane on the activation energy for a Si-Ge exchange.

different chemical identity of the other first neighbor atoms. We find that the activation energy increases as the number of Ge first neighbors attached to the atoms to be exchanged increases. However, for a given number of Ge first neighbors, there is some scatter (0.02eV) in the activation energy which can be attributed to the detailed arrangements of these atoms.

3.4.3 Second neighbors

We computed the activation energy for the Si-Ge exchange in systems with the

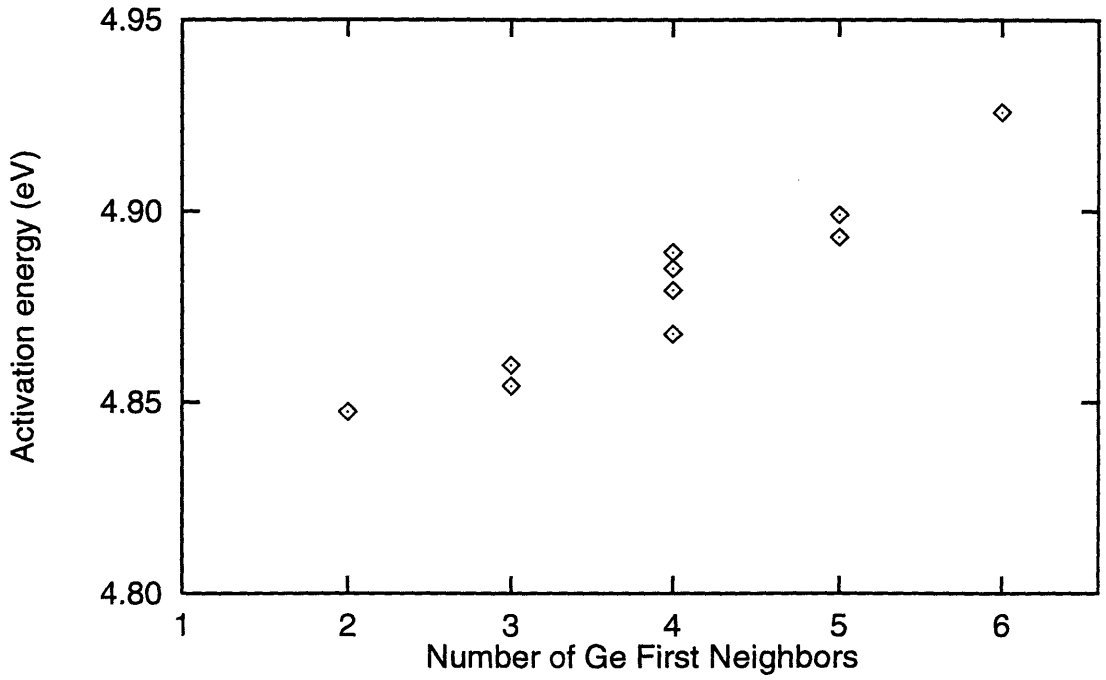

Figure 3-18: Effect of first neighbors (not on the preferred plane) on activation energy for structures with only Ge atoms attached to the atoms to be exchanged on the preferred unaffected plane.

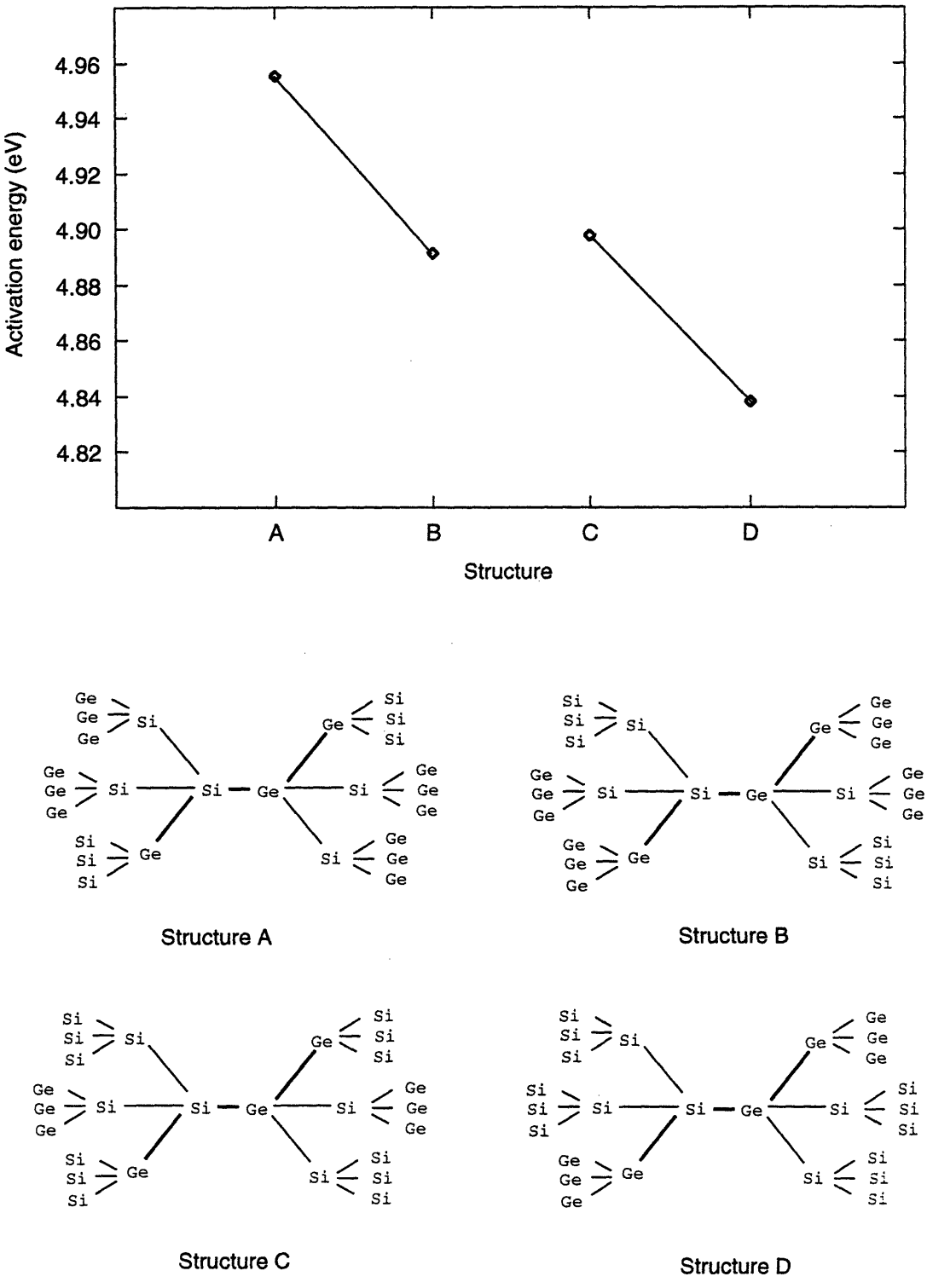

Figure 3-19: Effect of second neighbor environment on activation energy and schematic diagrams of structures with different second neighbor atom identities. The plane containing the atoms to be exchanged attached to the first neighbors through bonds shown in bold corresponds to the preferred unaffected plane.

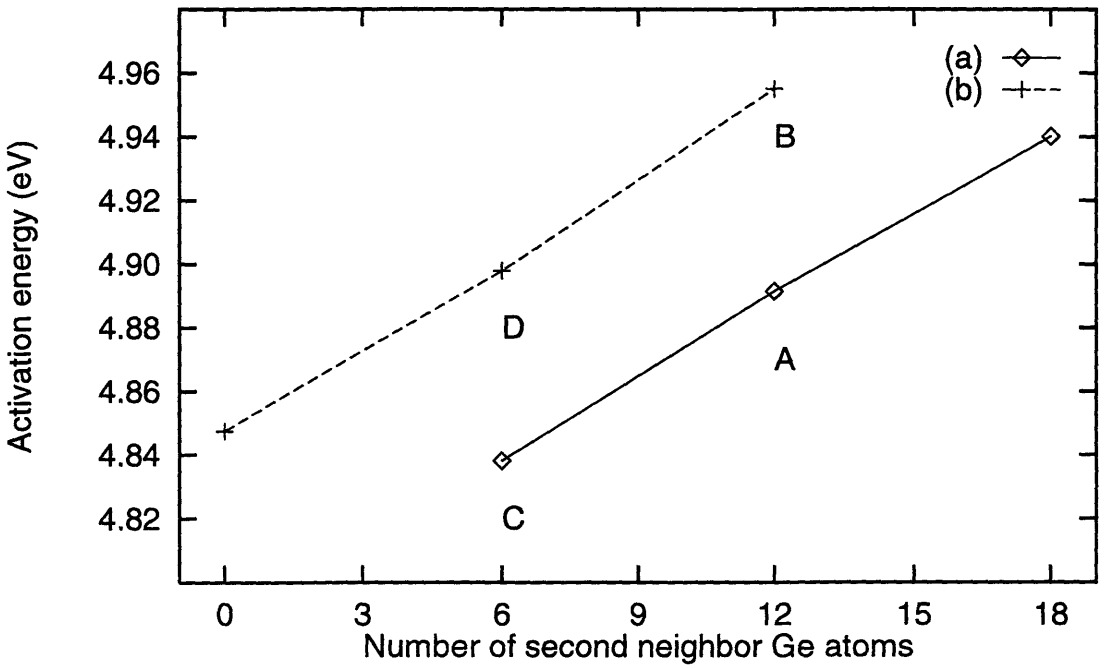

Figure 3-20: Effect of second neighbors on activation energy. (a) Ge second neighbor atoms attached to first neighbor atoms on preferred unaffected plane (b) Si second neighbor atoms attached to first neighbor atoms on preferred unaffected plane. Structures A,B,C and D are shown in Figure 3-19.

same first neighbor environment but with different second neighbor environments in an infinite Si matrix. Consider structures A and B (randomly labeled) that have 6 Si and 12 Ge second neighbor atoms as shown in Fig. 3-19. Structure A has only Ge second neighbor atoms attached to the atoms on the preferred unaffected plane and structure B has only Si second neighbor atoms attached to the atoms on the preferred unaffected plane. We find that a system with Ge atoms attached to the first neighbor atoms on the preferred unaffected plane (structure A) has a lower energy than a system with Si atoms attached to the first neighbor atoms on the preferred unaffected plane (structure B). A similar result is observed in structures C and D which have 12 Si and 6 Ge second neighbor atoms. Therefore, we conclude that two structures with the same number of second neighbors of a given chemical identity have different activation energies depending on the detailed arrangement of the atoms, i.e, the second neighbor atoms attached to the atoms on the preferred unaffected plane.

We found that in structures with the same chemical identity of second neighbor atoms attached to the atoms on the preferred unaffected plane, the activation energy increased with the number of second neighbor Ge atoms (Fig. 3-20). These trends are similar to the effect of the first neighbors on activation energy but smaller in magnitude. This is because the second neighbors are further away from the atoms to be exchanged.

So far we have only considered the effect of local environment on the activation energy for the exchange of a Si-Ge pair in a pure Si matrix. The next step is to study the effect of the chemical identity of the matrix (long range environment) on the activation energy.

3.4.4 Long range environment

We computed the activation energy for the Si-Ge exchange with various first neighbor environments in a Si matrix and in a Ge matrix. Two conclusions can be drawn from the results shown in Fig. 3-21). First, the changes in activation energy due to different first neighbor environments follow the same trend for diffusion in both a Si lattice and a Ge lattice. For example, there is a decrease in activation energy

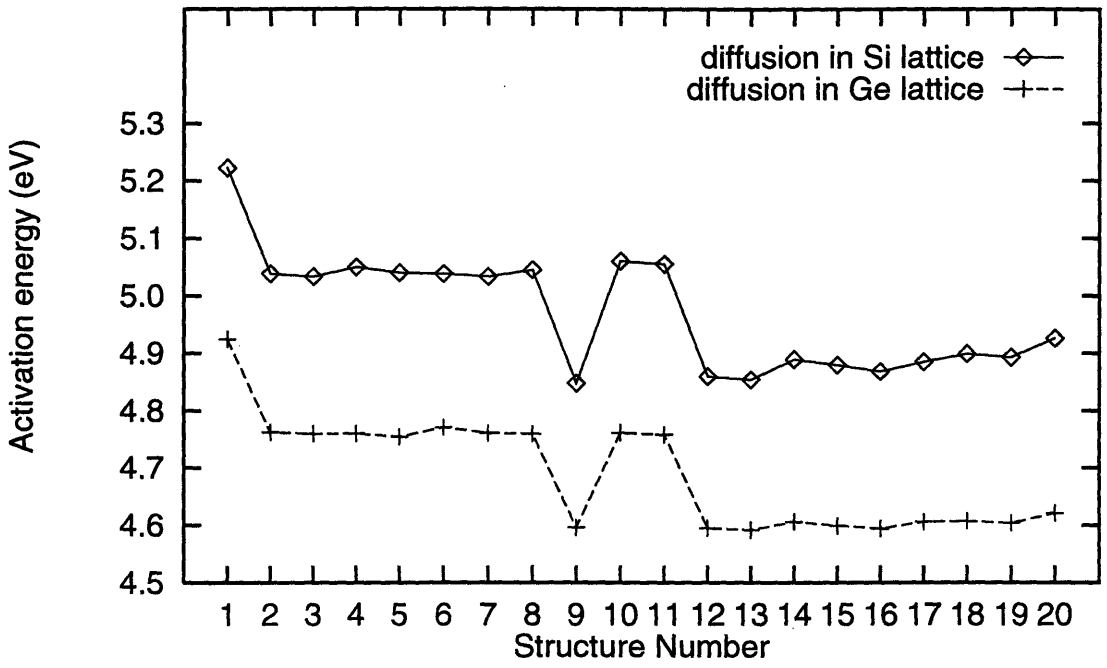

Figure 3-21: Effect of long range atom identity on activation energy. The activation energy for diffusion in a Ge lattice is lower than the activation energy for diffusion in a Si lattice.

when going from structure 8 to 9 for diffusion in Si lattice. A similar decrease is seen for the diffusion in Ge lattice. Also, the activation energies for diffusion in a Ge lattice are lower than in a Si lattice (Fig. 3-21). This is consistent with experimentally observed trends in activation energy for the diffusion of Ge dopants in a Si lattice and diffusion of Si dopants in a Ge lattice [48, 49, 50].

The results obtained so far shown the effect of the first neighbor environment (the presence of a preferred unaffected plane), the effect of the second neighbor and long range environment. In addition, the relative effect of these parameters on the activation energy has been clearly established. In any Si-Ge diffusion by the CE mechanism, the activation energy depends on the arrangement and chemical identity of the atomic environment of the atoms to be exchanged. Therefore, these results are applicable to any Si-Ge diffusion by the CE mechanism. In particular cases, in addition to these effects, the activation energy may depend on other factors. One such case is the nanocrystallite/host system where the effect of epitaxial strain has

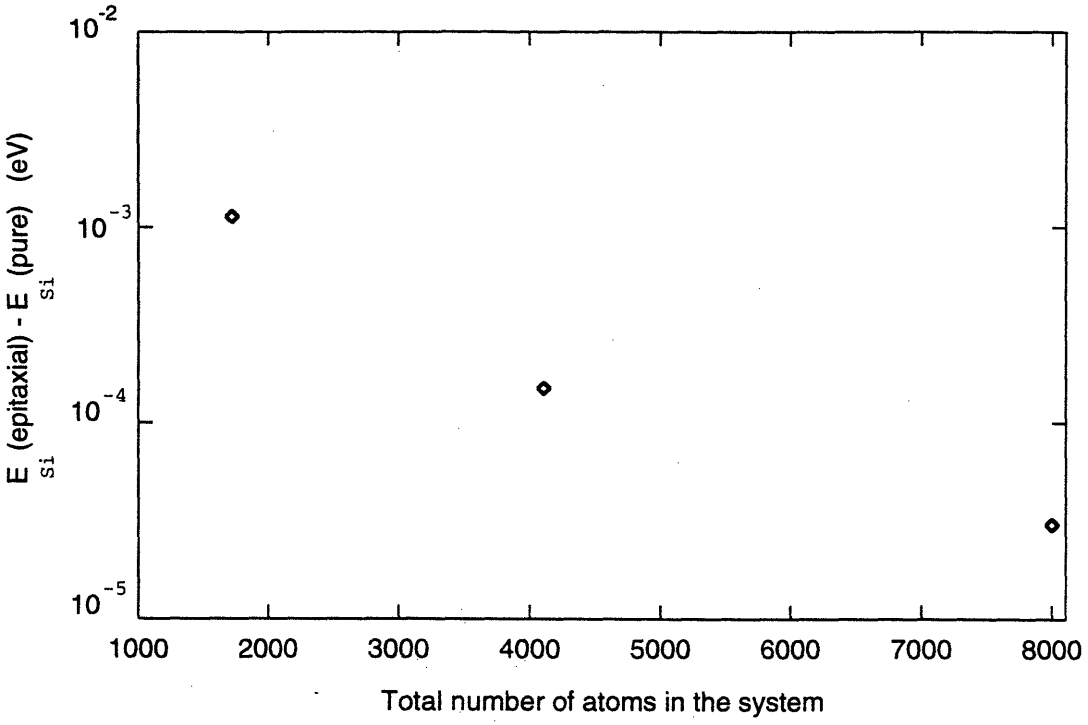

Figure 3-22: Converged system. $E_{Si}(epitaxial)$ is the contribution to total energy by the each additional Si atom in the next larger epitaxial system size. $E_{Si}(pure)$ is the contribution to total energy by a Si atom in a pure Si system

to be accounted for in the activation energy calculations. This particular case will be discussed in the following section.

3.5 Results: Epitaxial system

To study the effect of epitaxial strain on activation energy, we start from an initially relaxed system which contains a 10 Å Ge nanocrystallite (190 atoms) in an infinite Si host. In choosing the minimum host size, which for practical purposes be considered to be infinite, we sequentially consider epitaxial structures having the same number of Ge atoms but increasing number of Si atoms. In particular we considered systems with 512, 1728, 4096 and 8000 atoms. The energy of the epitaxial systems increases due to the addition of Si atoms. This increase in energy was averaged over the number of Si atoms added to the system. The average energy of the additional Si atom was compared with the energy of a Si atom in pure Si system. This was plotted

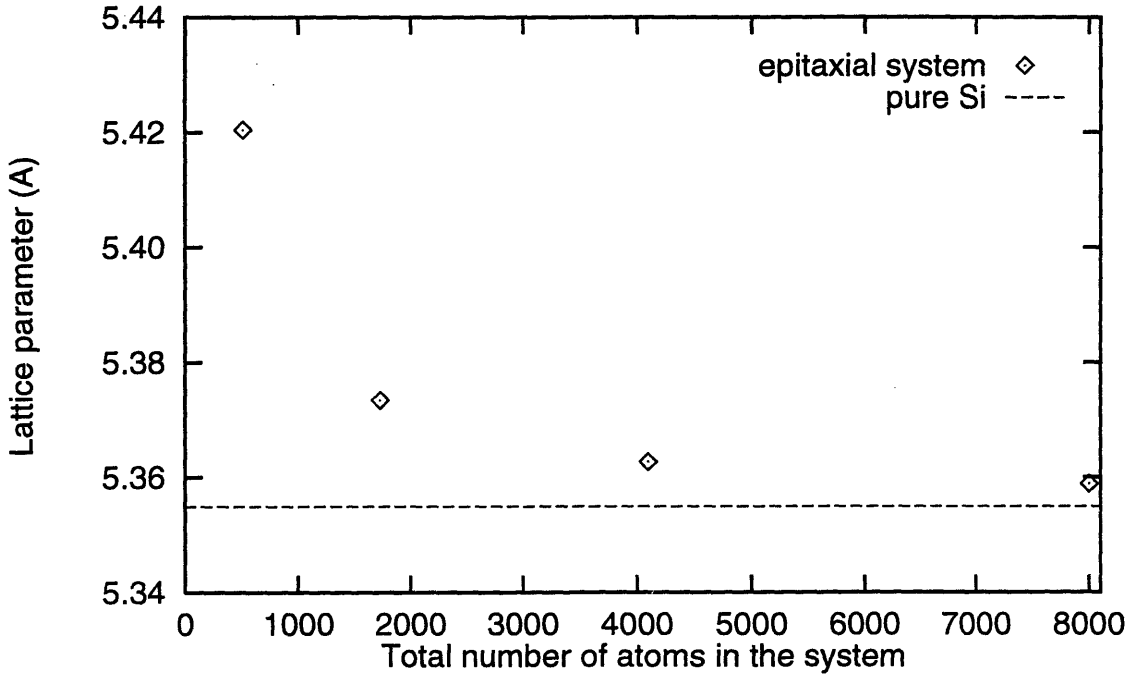

Figure 3-23: Converged system: The average lattice parameter of the 8000 atom epitaxial system is approximately equal to the lattice parameter of pure Si.

against the total number of atoms in the system in (Fig. 3-22). We found that, in the 8000 atom epitaxial system, the difference between the two energies was of the order of 10^{-5} eV. Therefore, the epitaxial system containing 8000 atoms was consid ered to equivalent to a Ge nanocrystallite in an infinite Si host. In addition, the average lattice parameter of the system was converged to the Si lattice parameter to within 0.005 Å in the 8000 atom system (Fig. 3-23).

3.5.1 Anisotropy in activation energy at the interface

We computed the activation energy for the exchange of atoms on the interface between the Ge nanocrystallite and the infinite Si host. The atoms to be exchanged were at approximately the same distance from the center of the nanocrystallite. We chose atoms that had the same preferred unaffected planes to be the atoms to be exchanged. We define the *exchange angle* as the angle at which the Si exchanges with a nearest neighbor Ge with respect to the radial direction as shown in Fig. 3-24. This direction

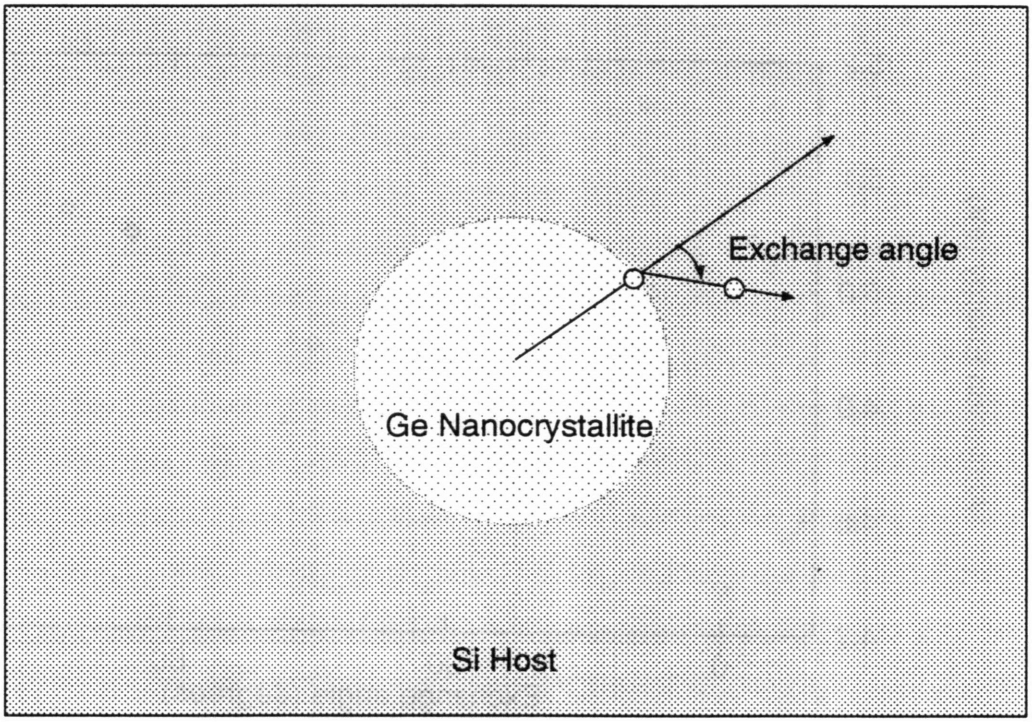

Figure 3-24: Exchange angle: The angle at which the Si exchanges with a nearest neighbor Ge with respect to the radial direction from the center of the nanocrystallite.

uniquely defines the local environment because of the spherical symmetry of the geometry.

We found that the activation energy is anisotropic and increases almost linearly with the exchange angle (Fig. 3-25). This indicates that exchanges in the radial direction are more favorable than exchange in the tangential direction. We attribute this anisotropy in activation energy to the presence of the Ge nanocrystallite at the center of the Si host. The coherent epitaxial Ge nanocrystallite at the center of the Si host is under compression while the Si host is under tension. The stress fields are such that the Si atoms are further apart in the tangential direction than in the radial direction. In reaching the activated state, the atoms to be exchanged rotate by an angle $\theta = 90°$ in the plane of the atoms to be exchanged and two first neighbors attached to them and by an angle of $\phi = 30°$ as explained in Section 2.2. Therefore, for a radial exchange the atoms to be exchanged rotate to the tangential position in the activated state. At this position, more space is available for the atoms to relax

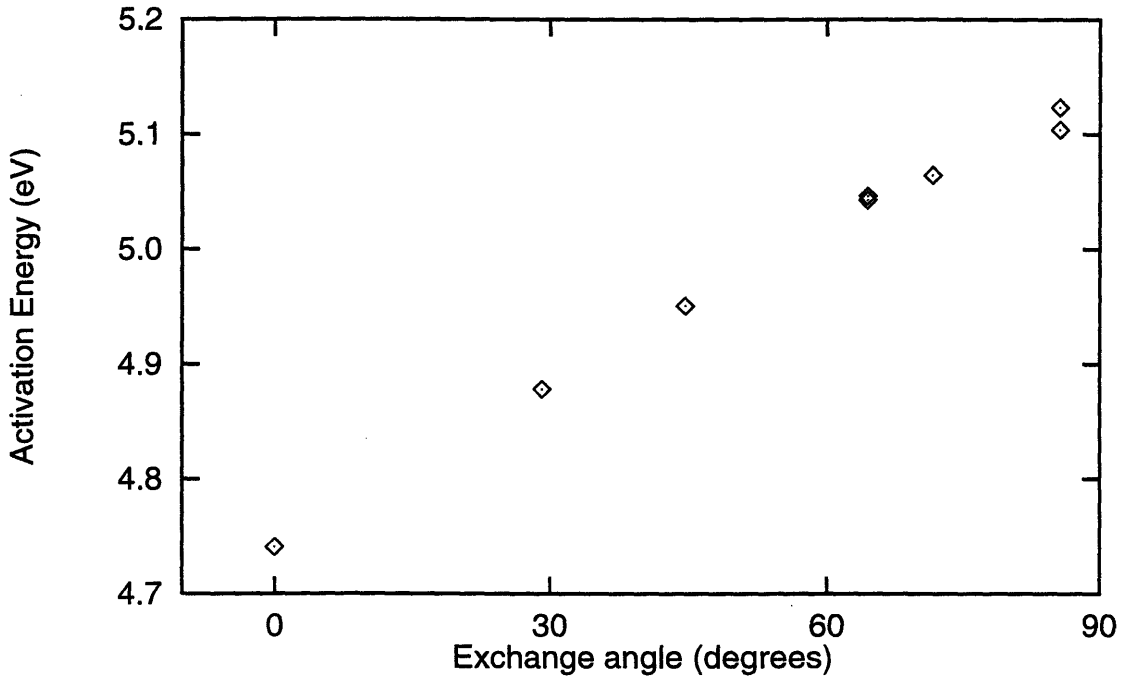

Figure 3-25: Anisotropy in activation energy: The activation energy for a radial exchange is lower than the activation energy for a tangential exchange.

and hence this activated state has a lower energy than others. The exchange along the radial direction lowers the strain more than any other exchange angle and hence the radial direction has the lowest activation energy.

3.5.2 Effect of strain on anisotropy in activation energy away from the nanocrystallite host interface

We computed the activation energy for the Si-Ge exchange in the Si matrix at various distances from the center of the nanocrystallite. The atoms to be exchanged had the same preferred unaffected plane (Si-Si). We found that the anisotropy in activation energy decreased on moving away from the interface (Fig. 3-26). This can be attributed to the decrease in strain (due to the nanocrystallite) on moving away from the interface.

the number of Ge first neighbors attached to the atoms to be exchanged. The effect of second neighbor environment on activation energy showed the same trend as the first neig hbors, but of a smaller magnitude. The activation energy was also found to depend on the chemical identity of the diffusing medium (long range environment). The activation energy for a Si-Ge exchange in a Ge matrix was lower than in a Si matrix.

We have investigated the effect of atomic environment on activation energy. In an epitaxial system, in addition to these effects, strain plays an important role. We find that the activation energy is anisotropic with respect to the exchange angle. We conclude that diffusion in the radial direction is favored against diffusion in the tangential direction. Also, on moving away from the Ge-Si interface, we find that the anisotropy in activation energy decreases as strain decreases.

We have studied the effect of environment and strain on activation energy. The most important insight this study provides is the relative order in which atoms diffuse out from the Ge nanocrystallite into the Si host. Given various configurations around the atoms to be exchanged, we can predict relative order of activation energies. From a knowledge of this and the effect of strain on activation energy, we can simulate diffusion in an actual system.

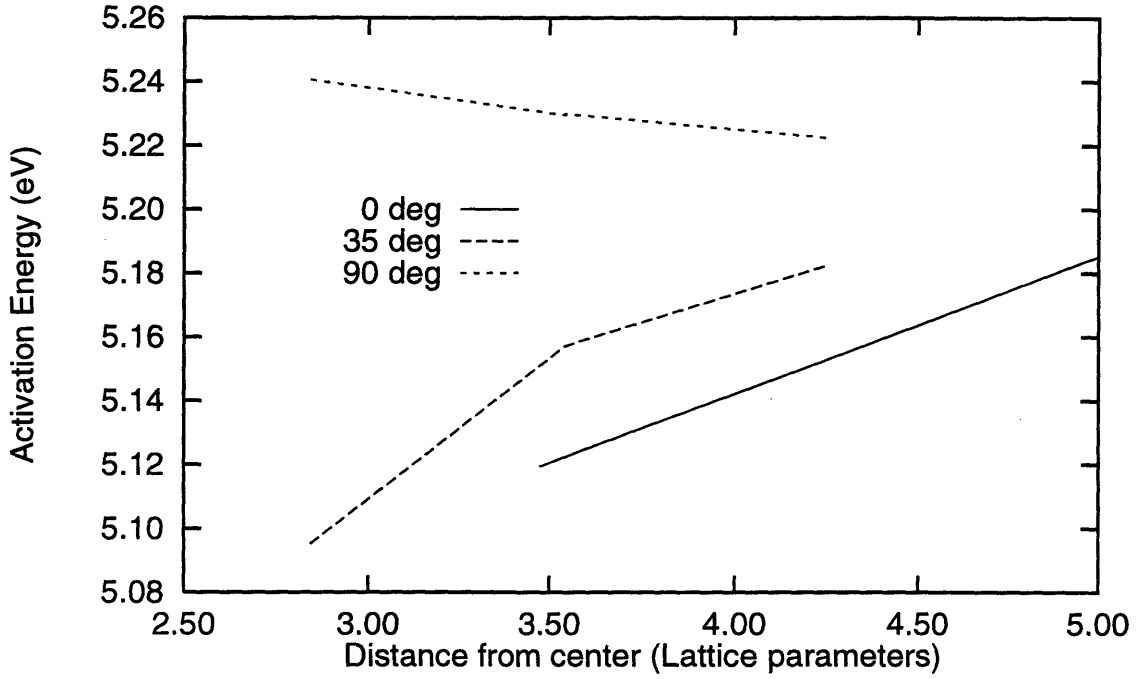

Figure 3-26: Effect of strain on anisotropy in activation energy away from the nanocrystallite/host interface

3.6 Conclusions

We have developed an energy model based on multi-body potentials to predict the effect of various parameters, such as strain and local environment, on activation energy for diffusion of Ge in Si by the concerted exchange mechanism.

We conclude that in this model the activation energy for interdiffusion in a given diffusing medium (e.g. Si matrix or Ge matrix) can be calculated accurately (to within 0.01 eV) by considering the effect of first and second neighbor environments. Depending on the first neighbor environment, there exists a "preferred unaffected plane" in reaching the activated state that is chosen based on energetic considerations. A Ge-Ge unaffected plane is preferred to a Si-Ge unaffected plane to a Si-Si unaffected plane. Depending on the preferred unaffected plane the activation energy could differ by 0.2 eV. For a given preferred unaffected plane. the chemical identity of the other first neighbor atoms (not on the preferred plane) have a much smaller impact (up to 0.07 eV) on the activation energy. The activation energy was found to increase with

Bibliography

[1] F.C. Frank and J.H. van der Merwe. *Proceedings of the Royal Society A*, 198:205, 1949.

[2] F.C. Frank and J.H. van der Merwe. *Proceedings of the Royal Society A*, 198:216, 1949.

[3] F.C. Frank and J.H. van der Merwe. *Proceedings of the Royal Society A*, 200:125, 1949.

[4] F.C. Frank and J.H. van der Merwe. *Proceedings of the Royal Society A*, 201:261, 1949.

[5] J.H. van der Merwe. *Journal Applied Physics*, 34:117, 1963.

[6] J.H. van der Merwe. *Journal Applied Physics*, 34:123, 1963.

[7] J.W. Matthews and W.A. Jesser. *Philosophical Magazine*, 15:1097, 1967.

[8] J.W. Matthews and W.A. Jesser. *Philosophical Magazine*, 17:461, 1968.

[9] J.W. Matthews and W.A. Jesser. *Philosophical Magazine*, 17:595, 1968.

[10] S.-T. Ngiam, K.F. Jensen, and K.D.Kolenbrander. Growth, processing and characterization of semiconductor heterostructures. volume 326, page 263, Boston, 1994. Materials Research Society Symposium Proceedings.

[11] M. Danek, K.F. Jensen, C.B. Murray, and M.G. Bawendi. *Applied Physics Letters*, 65:2795, 1994.

[12] M. Danek, K.F. Jensen, C.B. Murray, and M.G. Bawendi. Growth, processing and characterization of semiconductor heterostructures. volume 326, page 275, Boston, 1994. Materials Research Society Symposium Proceedings.

[13] S.-T. Ngiam, K.F. Jensen, and K.D.Kolenbrander. *Journal Applied Physics*, 76:8201, 1994.

[14] N.F. Mott and F.R.N. Nabarro. *Proceedings of Physics Society*, 52:86, 1940.

[15] F.R.N. Nabarro. *Proceedings of the Royal Society A*, 175:519, 1940.

[16] W.A. Jesser. *Philos. Magazine*, 19:993, 1969.

[17] L.M. Brown, G.R. Woolhouse, and U. Valdre. *Philos. Magazine*, 17:781, 1967.

[18] L.M. Brown. *Philos. Magazine*, 10:441, 1964.

[19] J.W. Matthews. *Journal of Vacuum Science and Technology*, 12:126, 1975.

[20] J.W. Matthews, S. Mader, and T. Light. *Journal of Applied Physics*, 41:3800, 1970.

[21] D. Houghton, D. Perovic, J.-M. Baribeau, and G. Weatherly. *Journal of Applied Physics*, 67:1850, 1990.

[22] S. Suresh, A.E. Giannakopoulos, and M. Olsson. Elastoplastic analysis of thermal cycling - layered materials with sharp interfaces. *JOURNAL OF THE MECHANICS AND PHYSICS OF SOLIDS*, V42:979, 1994.

[23] J.D. Eshelby. *Proceedings of the Royal Society, Series A*, 241:376, 1957.

[24] W.M. Lai, D. Rubin, and E. Krempl. *Introduction to Continuum Mechanics.* Pergamon Ress, New York, 1993.

[25] J.P. Hirth and J. Lothe. *Theory of Dislocations.* John Wiley & Sons, New York, 1982.

[26] J.W. Matthews. *Epitaxial Growth , Part B.* Academic Press, New York, 1975.

[27] G. Simmons and H. Wang. *Single Crystal Elastic Constants, 2nd Ed.* MIT Press, Cambridge, MA, 1971.

[28] A. Gomez, D.J.H. Cockayne, P.B. Hirsch, and V. Vitek. *Philos. Magazine*, 31:105, 1975.

[29] E.A. Fitzgerald. *Materials Science Reports*, 7:87, 1991.

[30] H. Foll and C.B. Carter. *Philos. Magazine*, 40:497, 1979.

[31] P. Zaumseil, U. Jagdhold, and D. Kruger. X-ray in situ observation of relaxation and diffusion processes in $Si_{1-x}Ge_x$ layers on silicon substrates. *Journal of Applied Physics*, 76:2191–6, 1994.

[32] M.L. Green, B.E. Weir, D. Brasen, Y.F. Hsieh, and others. Mechanically and thermally stable Si-Ge films and heterojunction bipolar transistors grown by rapid thermal chemical vapor deposition at 900 degrees C. *Journal of Applied Physics*, 69:745–51, 1991.

[33] W. Frank, U. Gosele, H. Mehrer, and A. Seeger. *Diffusion in Silicon and Germanium.* Diffusion in crystalline solids. Academic Press, New York, 1984.

[34] K.C. Pandey. Diffusion without vacancies or interstitials: a new concerted exchange mechanism. *Physical Review Letters*, 57:2287–90, 1986.

[35] R. Biswas and D.R. Hamann. New classical models for silicon structural energies. *Physical Review B (Condensed Matter)*, 36:6434–45, 1987.

[36] R. Biswas and D.R. Hamann. Interatomic potentials for silicon structural energies. *Physical Review Letters*, 55:2001–4, 1985.

[37] F.H. Stillinger and T.A. Weber. Computer simulation of local order in condensed phases of silicon. *Physical Review B (Condensed Matter)*, 31:5262–71, 1985.

[38] Z. Jian, Z. Kaiming, and X. Xide. Modification of Stillinger-Weber potentials for Si and Ge. *Physical Review B (Condensed Matter)*, 41:12915–18, 1990.

[39] J. Tersoff. Empirical interatomic potential for silicon with improved elastic properties. *Physical Review B (Condensed Matter)*, 38:9902–5, 1988.

[40] J. Tersoff. New empirical approach for the structure and energy of covalent systems. *Physical Review B (Condensed Matter)*, 37:6991–7000, 1988.

[41] E. Kaxiras and K.C. Pandey. New classical potential for accurate simulation of atomic processes in Si. *Physical Review B (Condensed Matter)*, 38:12736–9, 1988.

[42] B.W. Dodson. Development of a many-body tersoff-type potential for silicon. *Physical Review B (Condensed Matter)*, 35:2795–8, 1987.

[43] N. Toupance. Temperature dependence of the elastic constants for solids of cubic symmetry. Application to germanium and silicon. *Physica Status Solidi B*, 140:361–8, 1987.

[44] J.E. Bernard and A. Zunger. Strain energy and stability of Si-Ge compounds, alloys, and superlattices. *Physical Review B (Condensed Matter)*, 44:1663–81, 1991.

[45] A.F. Kohan and G.D. Garbulsky. *Private communication*, 1995.

[46] J. Gale. General utility lattice program. *version 1.0*, 1995.

[47] A. Qteish and R. Resta. Microscopic atomic structure and stability of Si-Ge solid solutions. *Physical Review B (Condensed Matter)*, 37:1308–14, 1988.

[48] J.H. Albany, editor. *International Conference on Defects and Radiation Effects in Semiconductors*, volume 46, Bristol, UK, 1979. Inst. Phys.

[49] M. Ogino, Y. Oana, and M. Watanabe. The diffusion coefficient of germanium in silicon. *Physica Status Solidi A*, 72:535–41, 1982.

[50] J. Raisanen, J. Hirvonen, and A. Anttila. The diffusion of silicon in germanium. *Solid-State Electronics*, 24:333–6, 1981.

2309-38